UNIVERSITÀ DEGLI STUDI DI SASSARI

XXI CICLO DI DOTTORATO

SCUOLA DI DOTTORATO IN SCIENZE BIOMEDICHE

ELASTOGRAFIA EPATICA: METODICHE A CONFRONTO

Coordinatore:
Prof. Andrea Piana

Tutor:
Dott. Gianpaolo Vidili

Tesi di Dottorato di:
SEBASTIANA MARIA ATZORI

CONTENTS

LIST OF ABBREVIATIONS

ARFI – Acoustic Radiation Force Impulse

ROI – Region of Interest

RTE – Real-Time Elastography

SWE– Shear-Wave Elastography

SR – Strain Ratio

SRI – Strain Rate Imaging

SSI – Supersonic Shear Imaging

TE –Transient Elastography

US – Ultrasonography

VCS – Visual Categorical Score

OVs - Oesophageal varices

LS - liver stiffness

NAFL **-** non-alcoholic fatty liver

NASH – non-alcoholic steatohepatitis

NAS - NAFLD activity score

pSWE - Point shear-wave elastography

2-D SWE – 2-dimensional shear-wave elastography

HVPG - pressure gradient of the hepatic vein

Kilo Pascal - kPa

Metres per second - m/s

AUROCs - (Area under the Received Curves)

ABSTRACT

Background: The cirrhotic process of liver injury is the end-stage of hepatic fibrosis, which results from progressive accumulation of extracellular matrix during the wound-healing response of the liver to repeated injury.

Mortality and morbidity rates increase exponentially once cirrhosis develops. Therefore, a prompt assessment of the degree of severity of fibrosis, an accurate and timely diagnosis of liver cirrhosis and management of complications are important in guiding therapy management in chronic liver disease. Liver biopsy is often required, but it is an invasive procedure, with a risk of severe complications (1/4000–10,000). In addition, its accuracy is prone to sampling error (6) and inter- and/or intra-observer diagnostic discrepancies occur in up to 10–20% of liver biopsies. For this reason, there is increasing interest in non-invasive methods for detecting liver fibrosis.

Ultrasound-based transient elastography (TE) is one of the first non-invasive imaging methods to be used in common practice. The technique is based on low-frequency vibrations: shear waves produced by the ultrasound machine propagate through the tissue and produce an elastic deformation, with the premise that liver stiffness (LS) measurements reflect the degree of hepatic fibrosis. Displacement is reflected in the variation of the acquired echo signals. The Siemens-based ARFI system and Philips Elast PQ^{TM} use conventional US to generate a shear wave directly within the liver tissues. This allows the sonographer to obtain both conventional US images and also specify a region of interest (ROI) for estimation of liver stiffness. The propagation velocity of the shear wave is reported in metres per second, and correlates with liver stiffness. The direct generation of shear wave within the liver tissue holds advantages over TE since it is not subject to chest/abdominal wall distortion of the waves.

Results: 110 consecutive patients with liver disease underwent a liver biopsy and liver stiffness assessment by Philips EPIQ 7^{TM} ultrasound system, Siemens Acuson (ARFI) ultrasound system,

and Echosens Fibroscan^{TM} (currently the best-validated technique). The results of these three imaging techniques were compared with histological results.

A direct, strong correlation was observed between LS values assessed by TE elastography by Elast PQ and Virtual Touch ($p < 0.0001$) and Metavir score.

LIVER DAMAGE

Hepatic fibrosis can be defined as a dynamic process involving cellular, molecular and tissue processes which leads to the accumulation of components of the cellular matrix (ECM) in the liver parenchyma [8]. The pathologies associated with the development of liver fibrosis include chronic infection by hepatotropic viruses (HBV and HCV), chronic exposure to toxic substances (the most common cause being alcohol misure), chronic exposure to altered metabolic conditions and damage caused by autoimmune alterations. The chronic liver damage caused by a chronic inflammatory response, combined with other pathogenetic mechanisms, such as oxidative stress, alteration of the relationship between mesenchymal and epithelial cells and the activation of fibrogenesis, leads to an unbalanced process which favours the formation of fibrous tissue [9-13]. The accumulation of extracellular matrix proteins determines a progressive alteration of the liver architecture, initially characterised by the formation of fibrous septa, as a result of regenerative nodules, with the subsequent development of cirrhosis. Cirrhosis causes hepatocellular dysfunction and determines an increase in resistance of hepatic blood circulation with the development of hepatic insufficiency and portal hypertension [14]. In most patients, the progression to cirrhosis occurs over a period of 15-20 years.

The main complications of cirrhosis include ascites, renal failure, hepatic encephalopathy and variceal bleeding. Patients with compensated cirrhosis do not develop complications for many years, whereas decompensated cirrhosis is associated with reduced survival; the only effective therapeutic strategy is liver transplant. Cirrhosis is also a risk factor for the development of hepatocellular carcinoma [15].

In recent years, substantial progress has been made in understanding the mechanisms that regulate fibrogenesis. In hepatic fibrosis hepatic stellate cells (HSCs), also called Ito cells or perisinusoidal cells, play a fundamental role, as an essential element for the production of collagen in the liver. This type of cell, described for the first time by Kupffer in 1876, undergoes a radical phenotypic

change in the presence of chronic liver disease, with consequent acquisition of fibrogenic properties [15]. In addition to hepatic stellate cells, portal myofibroblasts and bone marrow cells also appear to have fibrogenic potential [16].

The natural history of liver fibrosis is influenced by both genetic and environmental factors. The genes that regulate apoptosis and/or hepatocellular necrosis (Bcl-xL, Fas) affect the extension of liver damage and the subsequent fibrogenic response [17]. Genes regulating inflammatory response to liver injury (IL-1, IL 6, IL 10, IL-13, IFN, SOCS- 1 and osteopontin) determine the fibrogenic response to injury itself [17], while the genes that mediate the production of ROS (NADPH oxidase) regulate both inflammatory response and the deposition of extracellular matrix [18]. Fibrogenic growth factors (TGF-1, FGF), vasoactive substances (angiotensin II, norepinephrine) and adipokines (leptin and adiponectin) are necessary elements for the development of fibrosis [19]. Excess collagen removal is regulated by TIMP-1 and TGF-1 [20].

When the liver suffers an acute damaging stimulus, the parenchymal cells regenerate themselves and replace the necrotic or apoptotic cells. This process determines an inflammatory response and a limited deposition of extracellular matrix. If the damaging stimulus persists, the liver cells are no longer able to regenerate and the hepatocytes are replaced by abundant extracellular matrix, composed primarily of collagen fibres. The arrangement of the fibrous tissue depends on the type of damaging stimulus. In chronic viral liver disease and cholestatic hepatitis, fibrous tissue is localised initially in the portal spaces; in alcoholic liver disease it is localised in perisinusoidal areas [21].

Liver fibrosis is characterised by alterations in both the quantity and composition of the extracellular matrix. In advanced stages of fibrosis, the liver contains a quantity of extracellular matrix approximately six times higher than normal, predominantly consisting of collagen (I, III and IV), fibronectin, elastin, laminin, hyaluronic acid and proteoglycans. This extracellular matrix accumulation is caused by an increase in its synthesis and reduction in its degradation. The reduced activity of the metallo-proteinase (MMP), the enzymes responsible for extracellular matrix degradation, essentially depends on the increase in their specific inhibitors (TIMPs) [22].

Hepatic stellate cells (HSCs) are the main cells responsible for producing extracellular matrix in liver damage. In the normal liver, HSCs are localised in the space of Disse and store vitamin A. During liver injury, HSCs are activated and differentiate into fibrogenic and proliferating myofibroblasts [23]. Activated HSCs migrate and accumulate in the area of damaged tissue, producing a large amount of extracellular matrix and regulating its degradation. The Platelet-Derived Growth Factor (PDGF), produced primarily by Kupffer cells, is the most important mitogenic agent for HSCs. Collagen synthesis in HSCs is regulated both at the transcriptional level and the post-transcriptional [24]. The increase in collagen messenger RNA stability results in a greater production of this protein by activated HSCs [25].

In addition to hepatic stellate cells, other cell lines have fibrogenic potential. The myofibroblasts from small portal vessels proliferate around biliary tracts initiating collagen deposition in the liver fibrosis caused by cholestatic [26] disease. In addition, experiments on *in vitro* culture of hematopoietic stem cells CD34 + CD38- with different growth factor cells have led to the differentiation of hepatic stellate cells (HSCs) and myofibroblasts derived from bone marrow, able to localise in human liver tissue, resulting in remodelling of tissue architecture [27].

Moreover, the damaged hepatocytes produce reactive oxygen species (ROS) and fibrogenic mediators with consequent recruitment of inflammatory cells. Apoptosis of damaged hepatocytes stimulates collagen production by liver myofibroblasts [28]. The inflammatory cells, both polymorphonuclear and lymphocytic, activate the hepatic stellate cells with consequent production of collagen [29]. The activated hepatic stellate cells secrete inflammatory chemokines, express cell adhesion molecules and modulate the activation of lymphocytes [30]. In addition, the fibrogenic process is influenced by different subtypes of T helper lymphocytes present and the Th2 response is associated with an increased fibrogenesis [31]. Kupffer cells are resident macrophages that play an important role in liver inflammation by releasing ROS and cytokines [32]. Changes in extracellular matrix composition are able to directly stimulate fibrogenesis. Type IV collagen, fibrinogen and

urokinase-type plasminogen activator stimulate hepatic stellate cells through the activation of latent cytokines, such as TGF-1 [33].

The monocyte chemotactic protein-1 stimulates fibrogenesis, while IL-10 and IFN have the opposite effect [34]. Among the growth factors, TGF is a key mediator in human fibrogenesis, stimulating synthesis of extracellular matrix proteins and inhibiting their degradation [35]. The platelet-derived growth factor (PDGF) is the most important mitogen for hepatic stellate cells and its production increases in the fibrotic liver [36]. Cytokines with vasoactive properties regulate liver fibrogenesis. Substances that promote vasodilation (nitric oxide, relaxin) have antifibrotic effects, while substances that promote vasoconstriction (norepinephrine, angiotensin II) have the opposite effects [37]. Among the vasoactive cytokines, angiotensin II seems to play an important role in liver fibrogenesis; it is involved in liver inflammation and stimulates the proliferation and migration of hepatic stellate cells, the production of proinflammatory cytokines and collagen synthesis [39-40].

HISTOLOGICAL ASSESSMENT OF LIVER FIBROSIS

Histological assessment of the liver is able to quantify liver damage by identifying the necro-inflammatory grade or "grading" and the degree of fibrosis or "staging".

Grading

Grading is a histological evaluation of the necro-inflammatory state of the liver, and is identified by the following characteristics:

1. Quantity of inflammatory infiltrate (consisting of rare lymphocytes and plasma cells) in the portal tracts, hepatic artery and portal vein branches and biliary interlobular ducts within the fibrous matrix.

2. Quantity of periportal and lobular necrosis and destruction of hepatocytes induced by inflammatory cells (piecemeal necrosis).

3. Entities of confluent necrosis exceeding the limiting lamina and combining or forming bridges between vascular structures or, even more important, portals (bridging necrosis).

4. Quantity of degeneration of hepatocytes and focal necrosis within the lobule. All these data provide the histological grading of the disease [41, 42].

Staging

Staging is a histological evaluation of liver fibrosis and reflects the level of disease progression.

Semi-quantitative estimation of histological damage

In order to classify these histological alterations, the following standardised semi-quantitative scoring systems have been developed and are used in clinical practice.

Knodell

In 1981 Knodell and colleagues proposed a scoring system based on a numerical index of histological activity (Histology Activity Index, HAI). The model considers four separate scores for each component of the lesion: from 0 to 10 for periportal necrosis with or without bridging necrosis, 0 to 4 for intralobular degeneration and focal necrosis, 0 to 4 for portal inflammation, and 0 to 4 for fibrosis. The first three categories assess the intensity of inflammatory activity (grading) while the fourth indicates the degree of fibrosis (staging). In this model fibrosis scores are used on a discontinuous scale. Fibrosis is classified thus:

0 = absent

1 = fibrous portal expansion

3 = bridging fibrosis (porto-portal and porto-central)

4 = cirrhosis.

The main limitation of this system is that it groups necro-inflammatory activity and fibrosis, while these parameters describe different types of lesion and have different prognostic implications [43].

HISTOLOGICAL PATTERN	**SEVERITY**	**SCORE**
Periportal necrosis *piecemeal necrosis (PN)* *bridging necrosis (BN)*	Absent	0
	PN Mild	1
	PN Moderate	3
	PN Severe	4
	PN + BN Moderate	5
	PN + BN Severe	6
	Lobular necrosis	10
Intralobular necrosis	Absent	0
	Mild	1
	Moderate	3
	Marked	4
Portal inflammation	Absent	0
	Mild	1
	Moderate	3
	Severe	4

Fibrosis	Absent	0
	Portal tract expansion	1
	Bridging fibrosis	3
	Cirrhosis	4
Maximum score		22

Ishak

In1994 Ishak and colleagues proposed a revision of the Knodell model with some changes. This system uses a continuous scale of values that describes the degree of activity and the stage of fibrosis as two separate parameters [44]. Grading assessment is carried out separately, considering the different forms of necrosis and attributing a maximum score of 18 for the necro-inflammatory component. Staging evaluation is carried out using a continuous scale, giving a maximum score of 6 for cirrhosis.

HISTOLOGICAL PATTERN	**SEVERITY**	**SCORE**
Piecemeal necrosis	Absent	0
	Mild few mild focal areas)	1
	Mild/Moderate	2
	Moderate	3
	Severe	4
Confluent necrosis	Absent	0
	Focal confluent	1
	Zone 3 necrosis in some areas	2
	Zone 3 necrosis in most areas	3
	Zone 3 necrosis + occasional portal-central bridging	4
	Zone 3 necrosis + multiple P-C bridging	5
	Panacinar bridging	6

Focal lytic necrosis, apoptosis and focal inflammation	Absent	0
	One focus or less per 10 x objective	1
	2 to 4 foci	2
	5 to 10 foci	3
	More than 10 foci	4
Portal inflammation	Absent	0
	Mild, some or all portal areas	1
	Moderate, some or all portal areas	2
	Moderate/Marked, all portal areas	3
	Marked, all portal areas	4
	Maximum score	18

This system is less complex than the HAI and it can assess the portal/periportal component and the necro-inflammatory component separately.

Metavir

This classification system was proposed by the French cooperative study group METAVIR, and provided two separate scores for the evaluation of histological activity and fibrosis stage. It reflects the combination of lobular necrosis, portal inflammation, piecemeal necrosis and bridging necrosis. The activity ranges from 0 to 3. Fibrosis is classified into four stages [45].

HISTOLOGICAL PATTERN	**SCORE**
No fibrosis	0
Enlargement of portal tract without septa formation	1
Rare septa formation (> 1 septum)	2
Several septa	3
Cirrhosis	4

Non-alcoholic fatty liver (NAFL)

Steatosis is a result of excess accumulation of triglycerides in the liver. The threshold for considering steatosis as an abnormal feature is 5% hepatocytes. Steatosis is usually macrovesicular, but may be either purely large droplet or a mixture of small and large droplets (mediovesicular

steatosis). In macrovesicular steatosis, the lipid vacuole almost entirely fills the hepatocyte, pushing the nucleus to the side. Mediovesicular steatosis occurs when there are one or more smaller vacuoles in the cytoplasm. Microvesicular steatosis is a rare form in which the hepatocyte cytoplasm is replaced by innumerable small vacuoles, giving the cell a foamy appearance. True diffuse microvesicular steatosis is uncommon, but it may occur with patchy distribution in up to 10% of NAFLD. Steatosis may be distributed in a distinctly zone 3 (pericentral) centred pattern, but abundant steatosis can be panacinar, and when resolving, it may be irregular throughout the whole acinus. It is rare for steatosis to be localised in zone 1 (characteristic pattern of paediatric NAFLD), and as the disease progresses towards cirrhosis, steatosis may become more irregularly distributed or may vanish. A simple four-scale grading system (from 0 to 3) is used for grading steatosis. It takes into account only macro- and/or mediovesicular steatosis and assesses the percentage of hepatocytes decorated by steatotic vacuoles [19]. Normal liver (Grade 0) contains fat in < 5% of hepatocytes, while grade 1 steatosis refers to 33% steatotic hepatocytes. In grade 2 and 3 steatosis, fat is present in at least 33% or 66% of hepatocytes, respectively [46].

The relationship between steatosis and steatohepatitis is unclear. Although the natural history of NAFLD is still incompletely understood, it is clear that those who have the histological pattern of non-alcoholic steatohepatitis (NASH) and advanced fibrosis are at much greater risk of developing end-stage liver disease, liver-related mortality or extra-hepatic mortality than the general population of the same age and sex [47-48].

There are no non-invasive tests that can be performed to firmly identify patients with steatohepatitis or distinguish steatohepatitis from pure steatosis. Therefore, if there is a need to know with certainty whether or not a patient has NASH, a liver biopsy must be performed [49]. It is uniformly accepted that two cardinal features - lobular inflammation and liver cell clarification/ballooning - are mandatory features for NASH diagnosis. These patterns have been characterised best in the adult liver in which the lesions centre around the terminal hepatic vein, but once fibrosis progresses and parenchymal remodelling occurs, the lesions may lose preferential acinar localisation [50].

Inflammation is more often lobular in NASH, typically more prominent than portal inflammation in uncomplicated adult NAFLD. It consists mainly of clusters of mononuclear, but also Kupffer cells, microgranulomas with or without the lipid droplets, sometimes associated with hepatocyte dropout or apoptotic bodies. Neutrophil aggregates are rare and become prominent only if numerous Mallory–Denk bodies are present. The degree of lobular inflammation is usually mild and, when abundant, should suggest another or associated aetiology such as alcohol or drug toxicity [51].

Ballooned hepatocytes need to display both clear, flocculent, non-vacuolar cytoplasm, with a ballooned shape, as defined by the loss of the sharp angles of the liver cell. Size may or may not be increased compared to the size of normal hepatocytes. In the NAFLD activity score (NAS), ballooned cell grading is based mainly on number (none, few, many), while in the SAF score, it is mainly based on the size of ballooned cells.

Other features of hepatocellular injury may also be observed, such as apoptotic bodies, but they are usually sparse and inconstant. Mallory–Denk bodies may be present but they are less well-formed than in alcoholic hepatitis or alcoholic steatohepatitis and sometimes detected only by using p62 or ubiquitin immunohistochemistry. They can be numerous in severe NASH, but numerous Mallory–Denk bodies may suggest an associated alcoholic or toxic injury. The presence of Mallory–Denk bodies correlates with the histological severity of steatohepatitis and with other markers of progression and fibrosis in NASH [52].

NAFLD displays a continuous spectrum of steatosis, hepatocyte damage and inflammatory and fibrous lesions. Therefore, the categorisation of NAFLD into two subgroups (NASH, no NASH) is an oversimplification. Semi-quantitative scoring systems may partially avoid this limit.

NAFLD activity score (NAS)

NAS is based on the concept that necroinflammatory lesions and fibrosis stage should be separately evaluated, as the former is potentially more reversible than the latter. NAS was created as an unweighted score for steatosis (0–3), lobular inflammation (0–3) and ballooning (0–2).

Steatosis	0	< 3%
	1	5-33%
	2	33-66%
	3	>66%
Lobular inflammation	0	No foci
	1	< 2 foci/200x
	2	2-4 foci/200x
	3	> 4 foci/200 x
Hepatocyte ballooning	0	None
	1	Few balloon cells
	2	Many cells/prominent ballooning

SAF (Steatosis, Activity, Fibrosis) score

Steatosis	NAS Activity	Fibrosis
0-3	**0-8**	**0-4**
0 < 5 %	Steatosis 0-3	**0** Normal
1 5-33 %	+ Balloonisation 0-2	**1** Central
2 34-66%	+ Inflammation 0-3	**2** Central + portal
3 67-100%		**3** Septal fibrosis
		4 Cirrhosis

LIVER BIOPSY

Liver biopsy has long been the "gold standard" for the diagnosis, staging and follow-up of liver diseases and is currently the comparison method in comparative studies on the efficiency of non-invasive diagnostic markers of fibrosis. The biopsy for liver disease can be performed by the percutaneous, laparoscopic or transjugular approach.

INDICATIONS FOR LIVER BIOPSY [53]

• Multiple parenchymal liver disease

• Abnormal liver function tests of unknown origin

• Fever of unknown origin

• Focal or diffuse abnormalities in imaging studies

• Prognostic-staging of known parenchymal liver disease

• Management-developing treatment plans based on histologic results.

ABSOLUTE CONTRAINDICATIONS [53]

• Uncooperative patient

• Platelets <50,000/mm

• Severe coagulopathy

• Infectious diathesis of the liver parenchyma

RELATIVE [53]

Ascites

Possible vascular lesions

Amyloidosis

Hydatid disease

The percutaneous biopsy is the most rapid, secure and most widely used approach for studying, grading and staging diffuse liver disease. In addition, most of the centres now use echo-assisted or ultrasound-guided percutaneous biopsy with a significantly reduced number of complications [54,55,56,57].

After the liver biopsy, the patient must remain under observation for 6 hours. During that period clinical parameters including blood pressure and heart rate should be monitored. Liver biopsy is a procedure that can be performed in an outpatient setting. Liver biopsy complications rarely occur. 60% of complications occur within 2 hours and 96% within 24 hours of the procedure. A proportion of patients between 1% and 3% require hospitalisation for complications [58].

Minor complications include transient post-biopsy pain in the right hypochondrium area, experienced by patients in approximately 30% of cases, and the resulting transient hypotension with a vaso-vagal reaction. Major complications include intraperitoneal bleeding, subcapsular or intraparenchymal haematoma, haemobilia and accidental puncture of other organs such as the lung, kidney, gall bladder or colon, resulting in bile peritonitis, pneumothorax, subcutaneous emphysema, pleural effusion, haemothorax, sepsis or abscesses and haemoptysis [59]. With improved techniques and tools and ultrasound devices, the major complications have decreased substantially over time and currently range between 0.3% and 12.57% [60].

Post-procedure mortality varies from 0.01% to 0.17% and is mostly caused by bleeding in patients with cirrhosis or primitive malignant lesions of the liver [61]. Another important aspect to consider is the cost of this diagnostic procedure [62]. The main limitations of the histological assessment of liver biopsy are sampling error and variability in inter- and intra-observer interpretation. Sampling error is closely related to irregular distribution of liver damage and involves both staging and necro-inflammatory grading that is usually underestimated. The importance of sampling errors has recently been emphasised by one study on liver biopsies, obtained by the laparoscopic approach which showed differences in excess of one point of the fibrosis score according to Scheuer between

the left lobe and right lobe in about one third of cases (30.4 %); however in 14.5% of cases the diagnosis of cirrhosis was made in one lobe but, not the other [63].

Autopsy studies and laparoscopic comparison indicate that liver biopsy underestimates cirrhosis in 10-30% of cases, depending on the type of needle used and the size of the sample taken [64, 65]. Sampling error decreases in proportion to the increase in size of the biopsy specimen. Generally, for an accurate diagnosis a sample of liver 1.5-2.5 cm in length and 1.2-2 mm thick is necessary [46]. The importance of sample size is demonstrated by a study that showed that correct diagnosis is possible in 65% of cases with samples of 15 mm length and above 75% of cases with cores of 25 mm length [46]. The number of portal tracts in the sample is also very important; the sample must include at least eleven portal spaces [46].

PORTAL HYPERTENSION

Portal hypertension (PHT) is a clinical syndrome defined by a portal venous pressure gradient between the portal vein (PV) and inferior vena cava exceeding 5 mmHg [1]. Cirrhotic PHT is associated with an elevated hepatic venous pressure gradient (HVPG) predominantly due to raised sinusoidal resistance. non-cirrhotic PHT (NCPH), HVPG is normal or only mildly elevated and is significantly lower than PV pressure.

Non-cirrhotic Portal Fibrosis (NCPF) variously called as Idiopathic PHT (IPH), hepatoportal sclerosis and obliterative venopathy, is a disorder of unknown etiology, clinically characterized by features of PHT; moderate to massive splenomegaly, with or without hypersplenism, preserved liver functions, and patent hepatic and portal veins.

Rarity of the disease in the west, a declining trend with improved standards of living and hygienic conditions support the role of infections, of imprecise nature, at an early age in the disease pathogenesis. Role of prothrombotic disorders in the pathogenesis is supported by autopsy studies

showing high prevalence of PV thrombosis (PVT) and studies from the west indicating association with prothrombotic states. Immunological basis is propagated due to female preponderance, association with various immunological and autoimmune disorders, and presence in serum of various autoantibodies. phlebosclerosis, fibroelastosis, periportal, and perisinusoidal fibrosis, aberrant vessels in portal tract (portal angiomatosis), preserved lobular architecture, and differential atrophy. Main PV trunk is dilated with thick sclerosed walls, along with thrombosis in medium and small PV branches – the histological hallmark termed ‘‘obliterative portal venopathy’’. Long term survival after eradication of esophagogastric varices and after a properly timed shunt surgery is nearly 100% and 80%, respectively [17,101]. Liver functions usually remain well preserved, but with course of time in 20–33% of cases, liver slowly undergoes parenchymal atrophy with subsequent decompensation, development of HPS and need for LTx [102,103]. follow-up study, PVT, ascites and liver failure have been shown to develop in 46%, 50%, and 21%, respectively, over a mean period of 7.6 years – the later 2 complications were associated with variceal bleeding, surgery or concurrent extrahepatic disease [14]. Worsening of preexisting PHT and development of new PVT occurred in 46% and 28%, respectively, with a proportion requiring LTx [15]. Development of PVT is thus considered a major event contributing to progression of liver disease and eventual decompensation. However, the same has not been shown in the transplant and autopsy series

NON-INVASIVE METHODS FOR EVALUATION OF LIVER FIBROSIS

In recent years, research has focused on the evaluation of non-invasive methods for the assessment of liver fibrosis.

According to EASL guidelines, non-invasive methods are not merely an alternative to biopsy for staging fibrosis, but also predictive of the incidence of liver-related complications of liver fibrosis, including HCC development [66].

Non-invasive methods rely on two different approaches: a biological approach based on the quantification of biomarkers in serum samples or a "physical" approach based on the measurement of liver stiffness (LS).

SERUM MARKERS OF LIVER FIBROSIS

Serum markers of liver fibrosis are divided into direct and indirect markers. Indirect markers reflect the liver damage and include routine laboratory parameters such as GOT/AST transaminases and GPT/ALT, platelet count, gamma globulin, albumin, cholinesterase and INR. Direct markers reflect the changes in the extracellular matrix and enzymes. This category includes part of the glycoproteins, such as hyaluronic acid and laminin, collagens, such as procollagen III and collagen type IV and matrix metalloproteinases (MMPs) and their inhibitors (TIMPs). The advantage of serum markers is that they are universally available and reproducible. However, they can be influenced by comorbidities and medications that need to be considered when the results are interpreted. The table shows the different serum markers available.

HCV	
Fibrotest	patented formula combining α-2-macroglobulin, γGT, apolipoprotein A1, haptoglobin, total bilirubin, age and gender
Forns Index	7.811 - 3.131 x ln(platelet count) + 0.781 x ln(GGT) + 3.467 x ln(age) - 0.014 x (cholesterol)
AST to Platelet Ratio (APRI)	AST (/ULN)/platelet (109/L) x 100

FibroSpect II™	patented formula combining α-2-macroglobulin, hyaluronate and TIMP-1
MP3	0.5903 x log(PIIINP [ng/ml]) - 0.1749 x log(MMP-1 [ng/ml])
Enhanced Liver Fibrosis score™ (ELF)	patented formula combining age, hyaluronate, MMP-3 and TIMP-1
Fibrosis Probability Index (FPI)	10.929 + (1.827 x Ln[AST]) + (0.081 x age) + (0.768 x past alcohol use*) + (0.385 x HOMA-IR) –(0.447 x cholesterol)
Hepascore™	patented formula combining bilirubin, γGT, hyaluronate, α-2-macroglobulin, age and gender
Fibrometer™	patented formula combining platelet count, prothrombin index, AST, α-2-macroglobulin, hyaluronate, urea and age
Lok index	-5.56 - 0.0089 x platelet (103/mm3) + 1.26 x AST/ALT ratio = 5.27 x INR
Goteborg University Cirrhosis Index (GUCI)	AST x prothrombin - INR x 100/platelet
Virahep-C model	-5.17 + 0.20 x race + 0.07 x age (yr) + 1.19 ln(AST [IU/L]) - 1.76 ln(platelet count [103/ml]) + 1.38 ln(alkaline phosphatase (IU/L])
Fibroindex	1.738 - 0.064 x (platelets [104/mm3]) + 0.005 x (AST [IU/L]) + 0.463 x (gamma globulin [g/dl])
HALT-C model	-3.66 - 0.00995 x platelets (103/ml) + 0.008 x serum TIMP-1 + 1.42 x log(hyaluronate)
HBV	
Hui score	3.148 + 0.167 x BMI + 0.088 x bilirubin - 0.151 x albumin - 0.019 x platelet
Zeng score	-13.995 + 3.220 log(α-2-macroglobulin) + 3.096 log(age) + 2.254 log(GGT) + 2.437 log(hyaluronate)
HIV-HCV	
FIB-4	age (yr) x AST [U/L]/(platelets [109/L] x (ALT [U/L])1/2
SHASTA index	-3.84 + 1.70 (1 if HA 41-85 ng/ml, 0 otherwise) + 3.28 (1 if HA >85 ng/ml, 0 otherwise) + 1.58 (albumin <3.5 g/dl, 0 otherwise) + 1.78 (1 if AST >60 IU/L, 0 otherwise)
NAFLD	
NAFLD Fibrosis Score (NFS)	(-1.675 + 0.037 x age (yr) + 0.094 x BMI (kg/m2) + 1.13 x IFG/diabetes (yes = 1, no = 0) + 0.99 x AST/ALT ratio - 0.013 x platelet count (x109/L) - 0.66 x albumin [g/dl])
BARD score (BMI ≥28	
Steato Test™	ALT, A2M, ApoA1, haptoglobin, total bilirubin, GGT, total cholesterol, TG, glucose, age, gender and BMI
Fatty liver index (FLI)	BMI, TG, WC, and GGT

Hepatic steatosis index (HSI)	AST/ALT, BMI, and diabetes
Lipid accumulation product (LAP)	WC, TG and gender
Index of NASH (ION)	Male: waist-to-hip ratio, TG, ALT and HOMA Female: TG, ALT and HOMA
MS, diabetes, insulin, AST/ALT	

Table 1: A2M a2-macroglobulin, ALD alcoholic liver disease, ALT alanine transaminase, AST aspartate transaminase, ApoA1 apolipoprotein A-1, BMI body mass index, CHB chronic hepatitis B, CHC chronic hepatitis C, CLD chronic liver disease, GGT gamma-glutamyl transferase, LB liver biopsy, MRS magnetic resonance spectroscopy, MS metabolic syndrome, SLD suspected liver disease, TG triglycerides, US ultrasonography, WC waist circumference [71]

Several multi-parameter scores that combine direct and/or indirect serum markers were evaluated and some of these are commercially available. APRI (AST/platelet) and FibroTest™ have been studied the most. Two meta-analyses, which included 8,739 and 4,266 patients with chronic hepatitis C virus, reported good accuracy (> 80%) for the APRI in diagnosing significant fibrosis, but poor accuracy for the diagnosis of intermediate stages of fibrosis [67, 68]. APRI shows less diagnostic accuracy in the liver fibrosis stages caused by chronic HBV infection. The FibroTest™ consists of a combination of indirect markers. A meta-analysis that evaluated the diagnostic performance of FibroTest™ showed good diagnostic accuracy (> 80%) in diagnosing significant fibrosis (F METAVIR> 2) and liver cirrhosis (F = 4) in patients with chronic liver disease [69]. A study that included 1,307 patients with a viral infection (HCV 913, 284 HBV, HIV 110) and prospectively compared the FibroTest™, Fibrometer, Hepascore and APRI, showed no significant difference between the various diagnostic methods in the diagnosis of significant fibrosis (AUROC 0.72- 0.78) and liver cirrhosis (AUROC 0.77-0.86) [70]. Several algorithms using a combination of serological markers to optimise the staging of liver fibrosis were evaluated. In a study that included 2,035 patients with chronic liver disease, the use of a sequential combination of APRI and FibroTest™ (SAFE biopsy) led to a reduction of 47% in the biopsies for diagnosing significant fibrosis and 82% in the diagnosis of cirrhosis of the liver [70]. Other combinations of algorithms, such as Fibropaca (a simultaneous combination of FibroTest™, APRI and Forns-Index) and Leroy

(a simultaneous combination of APRI and FibroTest^{TM}) showed comparable results in patients with HCV-related chronic liver disease.

LIVER STIFFNESS IMAGING TECHNIQUES

Liver elasticity-based imaging techniques are divided into ultrasound-based techniques and 3-D magnetic resonance (MR) elastography [71].

Ultrasound elastography can currently be performed by different techniques, which are based on two physical principles: strain displacement/imaging and shear-wave imaging and quantification. Both strain elastography and SWE require mechanical excitation of tissue by manual compression (or cardiovascular pulsation and respiration), by the use of acoustic radiation force impulse (ARFI), or by a controlled external vibration. Strain elastography looks at the distribution of strain (measurement of tissue deformation) within a specified region of interest. SWE monitors the propagation of shear waves in tissues. The underlying principle for several, although not all, US-based techniques is that the velocity of a shear wave propagating through the liver is proportional to liver stiffness represented by the equation for Young' s elastic modulus E (E=3rv2), where v is shear velocity and r is tissue density, assumed to be constant. Shear waves propagate faster in stiffer tissue.

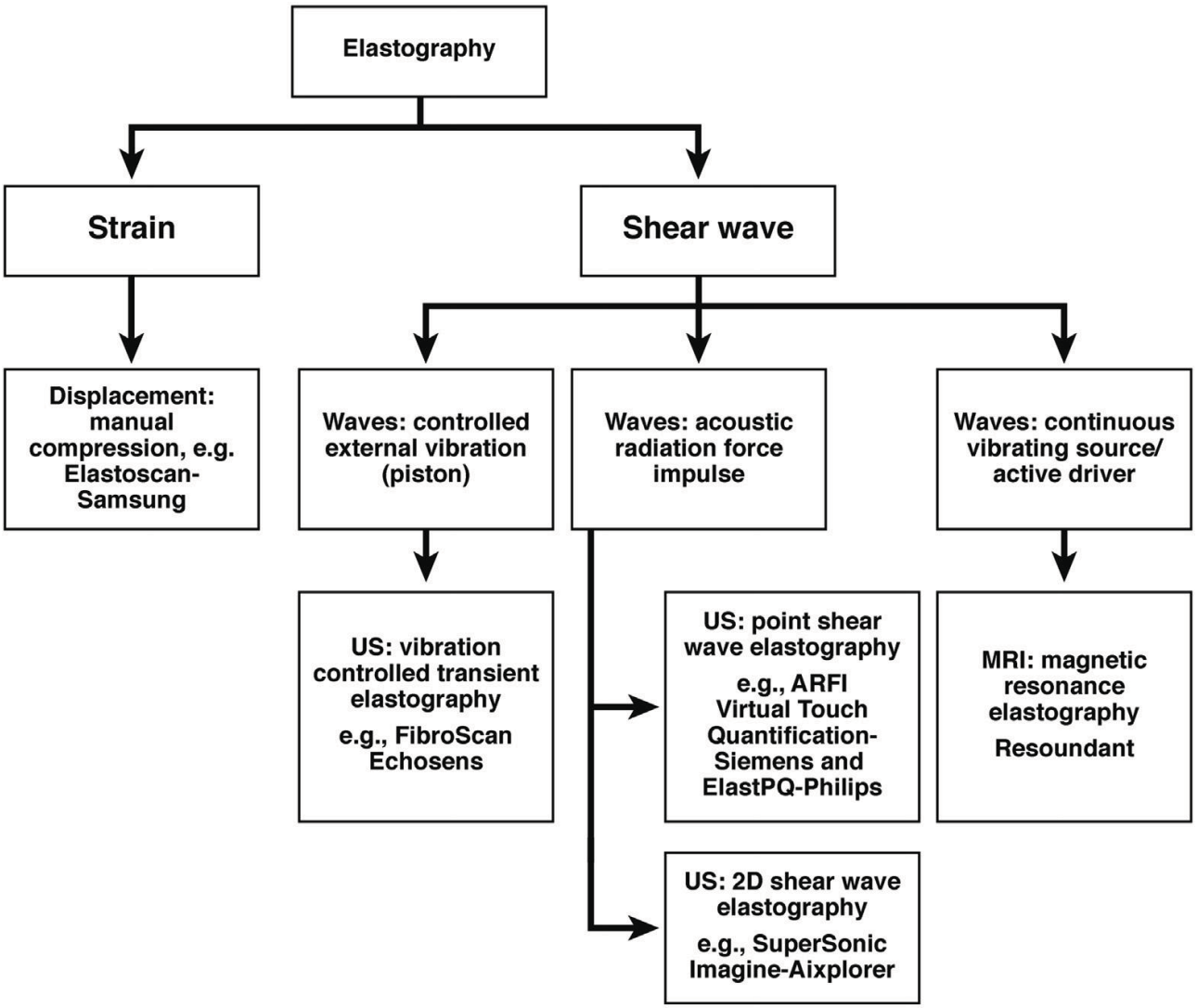

Figure 1: Principle of elastography methods [72]

Physical principles

Shear waves are transverse (i.e. the particle movement is across the direction of travel, as occurs in the ripples of a water surface when it is disturbed); they are rapidly attenuated by tissue; they travel slowly (between 1 and 10 m/s) and are not supported by low viscosity liquids. Their speed is related to Young's modulus of elasticity. Shear waves are produced by any mechanical disturbance and occur naturally from muscular movements (voluntary, cardiac etc.) as well as being induced by the ultrasound systems used to measure their speed.

There are three methods of shear-wave speed measurement in shear-wave elastography:

- Point shear-wave elastography (pSWE): a small measurement box (usually 5x10mm) is set up within the tissue and readings made of the shear-wave speed.
- 2-D shear-wave elastography: there are multiple sequential pushing and measurement points, so that a single static SWE image may be built up and displayed as a colour-coded map of the shear-wave speed which is quantitative (a ROI gives the readouts).
- Another form of elastography that is currently available also uses ARFI, but any shear wave generated is ignored and instead the amplitude of the displacement generated in the vicinity of the pushing beam's focus is displayed and used as a surrogate for the inverse of Young's modulus. Such displacement lasts only milliseconds and an image must be built slowly from multiple positions of the pushing focus, producing a qualitative static elastogram [73].

A dynamic force is mandatory for generating a shear wave. Elastography methods are divided into quasi-static methods and dynamic methods. When an ultrasound transducer is used to displace the tissue surface, this is referred to as quasi-static compression. It is caused by manual compression and decompression.

In dynamic methods an acoustic radiation force impulse induced by a high-energy ultrasound beam creates a shear wave or elasticity measured indirectly in kPa.

Ultrasound uses elastography images to observe the tissue deformation determined by shear waves. Pressure on the tissue surface causes a variation in density, and the perturbations generated travel together as a longitudinal wave. The longitudinal wave velocity cl (about $1540ms^{-1}$) is determined almost entirely by the density ρ of the tissue and the elasticity of compression modulus K. In an ideal situation (an elastically homogeneous medium of infinite spatial extent) the (transverse) shear-wave propagation speed cs is determined by ρ and the shear elastic modulus G. Because in soft tissues G is much smaller than K, shear waves travel about 1,000 times slower than longitudinal waves, typically in the range 1 – $10ms^{1}$. Unlike longitudinal waves, ultrasonic shear-wave frequencies are attenuated rapidly in soft tissue. Hence very low frequencies, often below 1 kHz

(which includes static deformations), must be used for elastography. Moreover, non-viscous pure fluids do not propagate shear waves [73].

All current commercial elastography systems need to measure shear-wave tissue displacement. The various systems differ in how the displacement is used; it may be measured directly, converted to strain, or used to detect the time of arrival of shear waves and hence their speed.

Measurements of the shear modulus G and its close relative Young's modulus E may be made non-invasively, if one can monitor the displacements of the tissue elements as a function of time as a shear wave passes multiple points along its path. For example, in TE and SWE, G is obtained from shear-wave speed measured as the difference in shear-wave arrival time at two or more points separated by known distances. In addition, both the percentage deformation (known as strain) and the displacement generated are directly dependent on the value of G for a given force, and both have been employed, in different elastography techniques, to display shear modulus contrast of tissues [73].

Quasi-static method

In quasi-static strain imaging, axial and lateral tracking is applied between each pair of RF-echo frames and the lateral displacements are discarded leaving a sequence of axial displacement images. Each axial displacement image is then converted into a strain image by passing a moving window (the strain-estimation window) down each image line, to calculate the local axial gradient of displacement at each window position. The size of the strain-estimation window is chosen as a compromise between strain image resolution (small window) and good strain signal-to-noise ratio [73].

Dynamic methods

Dynamic methods also use the tissue displacement estimation techniques employed in SE but differ in the method of applying the force or in the way that displacement is used. The localised displacement induced by a focused acoustic radiation force impulse may be displayed directly.

Alternatively, propagation of a transient displacement may be used to determine shear-wave speed. The dynamic nature of the force is essential in both cases.

Acoustic radiation force can create a localised displacement of a few microns in the ultrasound axial direction, which decays in a few ms [74]. Sufficient force for this purpose can be generated with a standard ultrasound scanner at depths of many centimetres by a sequence of rapid bursts of long focused ultrasound pulses [75]. The displacement is measured at a known time after cessation of the push using RF-echo tracking, and displayed as a qualitative elastogram within a small box [76].

Transient elastography employs a brief push (a small "thump") applied with an automated movement of the ultrasound transducer, which acts like a piston at the skin surface. The shear wave arises from the edge of the piston. A component of the wave converges on the ultrasound axis and after some distance travels down the axis at a speed close to the shear-wave speed. The shear displacement and depth is then measured using 1D correlation tracking methods, and the speed of the wave obtained from a displacement M-mode as the slope of a straight line. A special algorithm rejects displacement M-modes that are not linear enough. The shear-wave speed can be converted to a Young's modulus value using the relation E=3 ρcs 2, and the measurement given in kPa.

The system lacks 2D image guidance of the measurement, and it is not possible to propagate the shear wave beyond fluid collections (ascites). It may be difficult to obtain sufficient signals in obese patients with the standard probe (3.5 MHz, 2mm vibration amplitude), although the failure rate has been reduced by the introduction of a dedicated XL probe (2.5 MHz, 3mm vibration amplitude).

On the other hand, the use of the ribs for support when generating the intercostal transient shear wave limits the amount of prestress, which can be a confounding factor in elastography.

The transient surface displacement is also tightly controlled, as a single-cycle of a 50Hz wave. This is expected to help reproducibility of the measurements because tissue elasticity and hence shear-wave speed depends on the frequency of vibration. Finally, since the shear wave is not generated by

acoustic radiation force, it is relatively easy to keep the ultrasound thermal and mechanical indices low.

SWE can be used to produce two- or three-dimensional quantitative images of shear-wave speed with a useful field of view (2D SWE or 3D SWE).

The acoustic radiation force focus is swept down the acoustic axis, so as to generate tissue displacements. This produces a shear wave in the shape of a cone with a shallow angle (and hence almost cylindrical), known as a Mach cone, that travels away from the push line, which spreads less and thus decays less rapidly with distance than that from a single pushing focus. An ultrafast scanner achieves an ultrasound frame rate of up to 20 kHz by transmitting a plane wave and focusing only on receive, so that each ultrasound echo image is created with a single transmit pulse. This high frame rate allows the shear waves to be followed in real time in 2D, and RF-echo tracking over a grid of points produces a displacement movie and small map of shear-wave time-of-arrival can be created. The process is repeated for a number of different push lines to create a final quantitative elasticity image in a box, which is presented as a colour overlay on the B-mode image in units of ms-1, or converted to Young's modulus in kPa as for TE [77, 78]. The maximum size of the elastogram box is approximately 2–3 cm of side length with a linear transducer, and 9 x 4 cm with a convex transducer. Thus the system uses three frame rates: the standard B-mode echo image, a hidden ultrafast echo image used to track the displacement, and the shear-wave elastogram.

	method	type of force	applied force	property displayed	qualitative/ quantitative	imaging/ measure-ment	commercial implementation	illustration
displacement or strain imaging	strain elasto-graphy (SE) *and* strain-rate imaging (SRI)	quasi static	mechanically induced – *either* active external displacement of tissue surface[1] *or* passive internal physiologically induced[2]	strain or strain rate	qualitative, although tools often provided to analyse image characteristics	full area image, refreshed at up to the ultrasound frame rate[3]	Esaote GE Hitachi Aloka Philips Samsung Medison Siemens Toshiba Ultrasonix Zonare	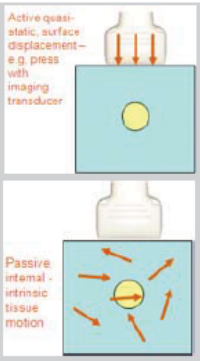
	acoustic radiation force impulse (ARFI) imaging	dynamic	ultrasound induced – focused radiation force impulse at depth	displace-ment	qualitative	single image within a box	Siemens	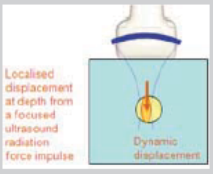
shear-wave speed MEASUREMENT	transient elasto-graphy (TE)[4]		mechanically induced – impulse ("thump") at tissue surface	shear-wave speed[5]	quantitative	single meas-urement, beam-line average	Echosens	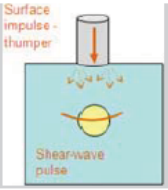
	point shear-wave elastography (pSWE), also known as ARFI quantification[4]		ultrasound induced – focused radiation force impulse at depth	shear-wave speed[5]	quantitative	single meas-urement, ROI average	Siemens Philips	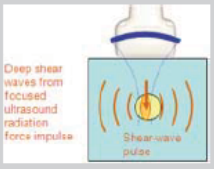
shear-wave speed IMAGING	shear-wave elas-tography (SWE)[4]		ultrasound induced – radiation force impulses focused at various depths	shear-wave speed[5]	quantitative	single image within a colour box	Siemens	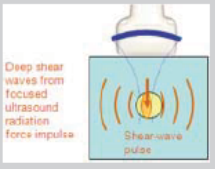
			ultrasound induced – radiation force focus swept over depth faster than shear-wave speed to create a Mach cone	shear-wave speed[5]	quantitative	image within a colour box, refreshed at up to several per second[3]	SuperSonic Imagine	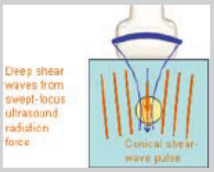

Table 2: Types of elastography [73]

TRANSIENT ELASTOGRAPHY

This is a one-dimensional ultrasonographic method that relies on the Fibroscan™ (Echosens, Paris, France) device, which measures the velocity of an ultrasound wave at low frequency (50 Hz) propagating through the liver. This speed is directly related to tissue stiffness.

TE was the first ultrasound-based elastographic technique for the liver, introduced in 2003, and has the largest body of evidence.

Fibroscan™ measurements are performed with the patient in the supine position; the probe is placed on the skin surface in a lateral position using a right intercostal approach (usually between the 9th and 11th intercostal spaces). The operator then presses the button located on the probe to perform the measurement. Liver stiffness measurement is performed in a cylinder approximately 1 cm wide by 4 cm in length at between 25 and 65 cm beneath the surface of the skin. The software determines whether the measurement was successful, and if so, the machine does not show a value on the display. The result is considered valid if ten valid measurements are performed: if the success rate (success rate, ratio of valid measurements and total number of measurements) is above 60%; if the interquartile range (IQR that reflects the variability of measurements) is less than 30% of the median (M) of the measurements (IQR/M <0.30%).

The results are expressed in kiloPascals (kPa) and vary between 1.5 and 75 kPa, with normal values around 7 kPa, and higher values in men and patients with low or high body mass index (body mass index, BMI) [79,80]. The advantages of Fibroscan™ are the speed of the procedure, the ability to have immediate results, and the possibility of testing both at the patient's bedside or in the clinic. It is also simple to use and can be performed by a nurse or technician after training. Nevertheless, Fibroscan™ results must be interpreted according to the patient's clinical presentation, hepatopathy aetiology and laboratory parameters. Although the Fibroscan™ has excellent inter- and intra-observer concordance (with an intra-class correlation coefficient of 0.98) [81,82], its accuracy is

lower in patients with higher transaminase levels. In the large case reported (13,369 examinations) [83], it was impossible to obtain a measurement result in 3.1% of cases, and in 15.8% of cases the results were not reliable (did not obtain the reliability criteria recommended by the manufacturer), mainly due to patient obesity or limited operator experience. Similar results were obtained in another study of 3,206 patients with a failure rate of 2.7% in measurements and an unreliability percentage of 11.6% [84].

Among the other parameters, IQR/M (Interquartile Range/Median) less than 30% has been suggested by the manufacturer to be the most important [85]. In one study [86] conducted on 1,165 patients, 798 of whom suffering from HCV-related chronic liver disease in which liver biopsy was used as the gold standard, in the multivariate analysis reliability of the results was tied to IQR/M increased to 30% and to liver stiffness measurement. It was observed that liver stiffness measurements higher than 7 kPa and IQR/M greater than 30% were associated with lower reliability of the results. However, higher reliability was observed in the group of patients with IQR/M lower than 30% regardless of the outcome of liver fibrosis. In order to reduce the number of patients with unreliable results due to obesity, a new probe was developed (XL, with 2.5 MHz transducer), enabling liver stiffness measurements at a depth between 35 and 75 mm [87, 88 89]. One study [89] conducted on 275 patients with chronic liver diseases (viral hepatitis 42%, 46% NAFLD) and BMI greater than 28 kg/m^2, showed that failure in obtaining results was less frequent when they used the XL probe, compared with the standard M probe (1.1% vs 16%; $p < 0.00005$). The study showed that unreliable results decreased with the XL probe in 25% of cases compared to 50% of cases with the M probe ($p < 0.00005$) and the values obtained with the XL probe were lower than those obtained with the M probe.

Fibroscan^{TM} results are also difficult to obtain in patients with narrow intercostal spaces and almost impossible in patients with ascites [90]. Moreover, inflammation, extrahepatic cholestasis or congestion can interfere with liver stiffness measurements. Confounding effects that can lead to overestimation have been noticed in increased transaminases, extrahepatic cholestasis, the presence

of congestive heart failure and food intake. For this reason, Fibroscan™ measurements should always be carried out with the patient having fasted for at least 2 hours [91-92-93-94]. The influence of steatosis on the results of Fibroscan™ measurements is still under debate. Although some studies have shown that there is a correlation between the degree of steatosis and liver stiffness levels measured by Fibroscan™ [95], more recent studies have denied this correlation [96, 97]. The Fibroscan™ was initially validated for the assessment of patients with HCV-related chronic liver disease. Subsequent investigations that have been conducted have validated this method for other chronic liver diseases. In HCV in chronic liver disease, levels greater than 6.8-7.6 kPa liver stiffness are related to the presence of significant fibrosis (F2). The cut-off values that predict the presence of cirrhosis are between 11.8 and 13.3 kPa [98,99,100,101].

With regard to chronic HBV-related liver disease a study of 202 patients showed cut-off values of 7.2 and 11 kPa, respectively, for significant fibrosis and cirrhosis [102]. The areas under the curve were respectively 0.81 and 0.93 for significant fibrosis and cirrhosis of the liver. A study conducted on 140 patients with HBV-related liver disease and 317 patients with HCV-related liver disease [103] showed a higher correlation in patients with chronic HCV-related liver disease: $r = 0.578$ vs $r = 0.408$ ($p = 0.02$). The average stiffness values of the liver measured by Fibroscan™ are similar for each stage of fibrosis in patients with chronic hepatitis B and C. However, a further study [104] conducted on 202 patients with chronic hepatitis C and 363 with chronic hepatitis B showed the same accuracy, sensitivity and specificity, and predictive value in patients with chronic hepatitis B and C. A study in an Asian population [105] showed that Fibroscan™-measured liver stiffness results were not affected by transaminase levels, while other studies showed a correlation [90]. In the studies conducted up to now, Fibroscan™ results have not been accurate in differentiating between contiguous stages of fibrosis (especially in the F1 and F2 stages) but have shown greater sensitivity in differentiating between the absence of significant fibrosis and fibrosis and between significant fibrosis and cirrhosis. A meta-analysis showed a cut-off value of 7.6 kPa (AUROC average of 0.84) for significant fibrosis and an optimum cut-off value of 13 kPa (0.94 AUROC

average) for cirrhosis [98]. In a further meta-analysis, the optimum cut-off values were 7.3 kPa and 15 kPa for significant fibrosis and cirrhosis, respectively [106].

In chronic alcohol-based liver disease, there is coexistence with inflammation and fibrosis can affect the liver stiffness results measured by Fibroscan^{TM}. Several studies have found higher cut-off levels, compared to those seen in patients with viral hepatitis for the diagnosis of cirrhosis (19.5 kPa, 22.6 kPa) [107]. However, in these studies the patients enrolled had elevated transaminase levels. A study of patients with alcoholic hepatitis showed that liver stiffness levels measured by Fibroscan^{TM} decreased with the reduction in transaminases [108]. A greater decrease was observed in particular with the reduction in AST and no significant increase in liver stiffness was observed for values of AST levels <100 U/L.

Several studies have shown that the Fibroscan^{TM} is considered an important tool in assessing the severity of C virus recovery in patients undergoing liver transplantation [109].

The Fibroscan^{TM} was also tested to evaluate complications of liver cirrhosis like portal hypertension. For the evaluation of portal hypertension the invasive detection of the hepatic venous pressure gradient (HVPG) remains the gold standard. A value greater than 10 mmHg can indicate the presence of clinically significant portal hypertension and a value higher than 12 mmHg may indicate the risk of bleeding from oesophageal varices [110]. In this study, the ROC curves for predicting portal hypertension were 0.945 with cut-off values of between 13.6 kPa and 21 kPa. Furthermore, the study observed greater correlation of the Fibroscan^{TM} measurements when HVPG measurement was less than 12 mmHg. Another study evaluated 100 patients with chronic liver disease performing HVPG and Fibroscan^{TM} measurements on the same day and following them up for the next two years. The study results showed that Fibroscan^{TM} measurement had similar accuracy to HVPG measurement in assessing the presence of portal hypertension (AUROC 0.830 vs 0.845) [111]. The cut-off proposed for estimating the presence of oesophageal varices in the various studies performed varied between 19.8 kPa and 47.5 kPa (AUROC 0.72-0.78) [112, 113]. A

further study showed different cut-off values in order to estimate the presence of oesophageal varices depending on the aetiology [114].

ACOUSTIC RADIATION FORCE IMPULSE (ARFI)

The acoustic radiation force impulse is a phenomenon associated with the propagation of acoustic waves in a medium of attenuation. The ARFI system is integrated within a conventional ultrasound, and the region of interest (ROI) for elastography measurement can be chosen under the B-mode vision. The tissue is stressed using an acoustic pulse that propagates through it. The energy transferred to the tissue by the acoustic impulse generates a deformation of the tissue itself. Soft tissues are more elastic and deform more than a rigid tissue whose deformability is lower. The deformation associated with the propagation of an ultrasonic pulse is then followed by a relaxation process, after which the tissue returns to its original position. ARFI elastography is used in the Siemens Acuson S2000^{TM} Ultrasound (Siemens AG, Erlangen, Germany) with a 4CI probe. The same principle is present in the Philips EPIQ^{TM}, Samsung, Hitachi and Esaote ultrasound systems. Results are expressed in metres per second (m/s). Like TE, this method gives better diagnostic results for liver cirrhosis and for the diagnosis of significant fibrosis. A meta-analysis that included 518 patients [115] with chronic liver disease (83% with chronic liver disease on a viral base) showed an AUROC value of 0.87 for the diagnosis of significant fibrosis, 0.91 for severe fibrosis and 0.93 for liver cirrhosis.

In another meta-analysis that included 36 studies (21 articles and 15 abstracts) for a total of 3,951 patients a value of 0.84 AUROCs was obtained and 0.91 for the diagnosis of significant fibrosis, severe fibrosis and liver cirrhosis, respectively [116]. The cut-off values suggested by the two meta-analyses were 1.34 to 1.35 m/s, 1.55-1.61 m/s, and 1.80-1.87 m/s for the diagnosis of significant fibrosis, severe fibrosis and liver cirrhosis, respectively. Studies comparing the two methods, Fibroscan^{TM} and ARFI, showed conflicting results. A recent meta-analysis [117] which included 13 studies with a total of 1,163 patients (11 articles and 2 abstracts) did not observe a significant

difference between the diagnostic reliability of ARFI and Fibroscan™. For the diagnosis of significant fibrosis, sensitivity and specificity were 0.74 and 0.83 for the ARFI, and 0.78 and 0.84 for the Fibroscan™, respectively. For liver cirrhosis diagnosis, sensitivity and specificity were 0.87 and 0.87 for the ARFI and 0.89 and 0.87 for the Fibroscan™, respectively. Reliable measurements were obtained in more patients with the ARFI system rather than with the Fibroscan™ (98% versus 93%, respectively, P <0.001).

REAL TIME SHEAR-WAVE ELASTOGRAPHY

Real-time shear-wave elastography is performed using the Aixplorer™ ultrasound system (SuperSonic Imagine S.A., Aix-en-Provence, France) with a convex probe (SC6-1) and it is also included in the GE and Toshiba ultrasound systems. In this method ultrasonic waves are created in the tissue by the radiant acoustic force generated by focused ultrasonic pulses. Ultrasonic waves then propagate through a given tissue and speed is then estimated using Doppler acquisition. The velocity of the sound waves can be used to calculate tissue stiffness by the formula $E = pc^2$, where E is tissue elasticity (in kilopascal, kPa), p is tissue density (kg/m^3) and c is the velocity of the tissue ultrasound waves (m/s). The speed estimate is then encoded using a colorimetric system by creating a quantitative image of two-dimensional shear wave tissue stiffness that is shown in a box in conventional B-mode images. The size and position of the shear-wave image is determined by the operator by positioning a circular region of interest (ROI) within the B-mode image. In addition to the tissue stiffness expressed in kPa, mean and standard deviation are calculated for the region of interest.

The first study published on this method that was compared with TE showed good diagnostic accuracy (AUROC 0.94 for significant fibrosis, 0.96 for severe fibrosis and 0.96 for cirrhosis) [118]. Another study [119] proposed a cut-off for F≥2 7.4 kPa (AUROC 0.91), for F≥3 8.7 kPa (AUROC 0.99) and for F = 4 9.2 kPa (AUROC 0.97).

ASSOCIATION BETWEEN FIBROSCAN AND SERUM MARKERS

Several algorithms have been proposed in which a combination of Fibroscan™ and serum markers must be used to evaluate liver fibrosis. An algorithm that considers Fibroscan™ and FibroTest™ (Castera/Bordeaux algorithm) was evaluated in order to optimise non-invasive diagnosis in patients with chronic hepatitis C [120]. According to this algorithm, if both methods are in agreement, hepatic biopsy is not needed; if liver biopsy is differentiated it could be ……should be performed. The combination of other elastographic methods and serum markers could be equally useful. Using such algorithms, biopsies could be reduced by 50-70%.

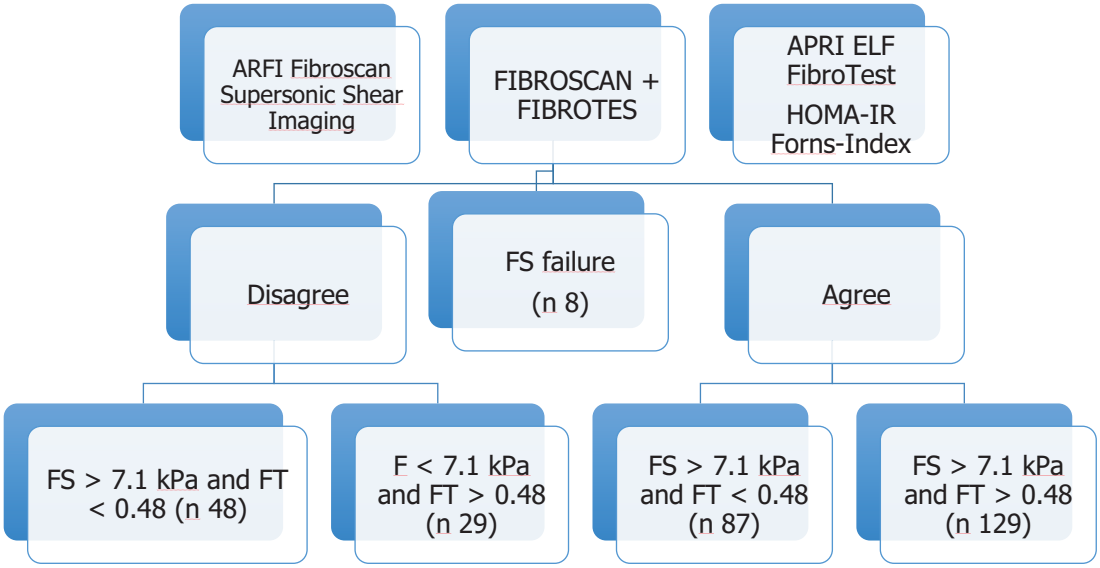

Figure 2: Castera/Bordeaux algorithm

For patients with chronic Hepatitis B several algorithms were proposed [121-122]. The proposed algorithm is summarised above in the EASL guidelines [73].

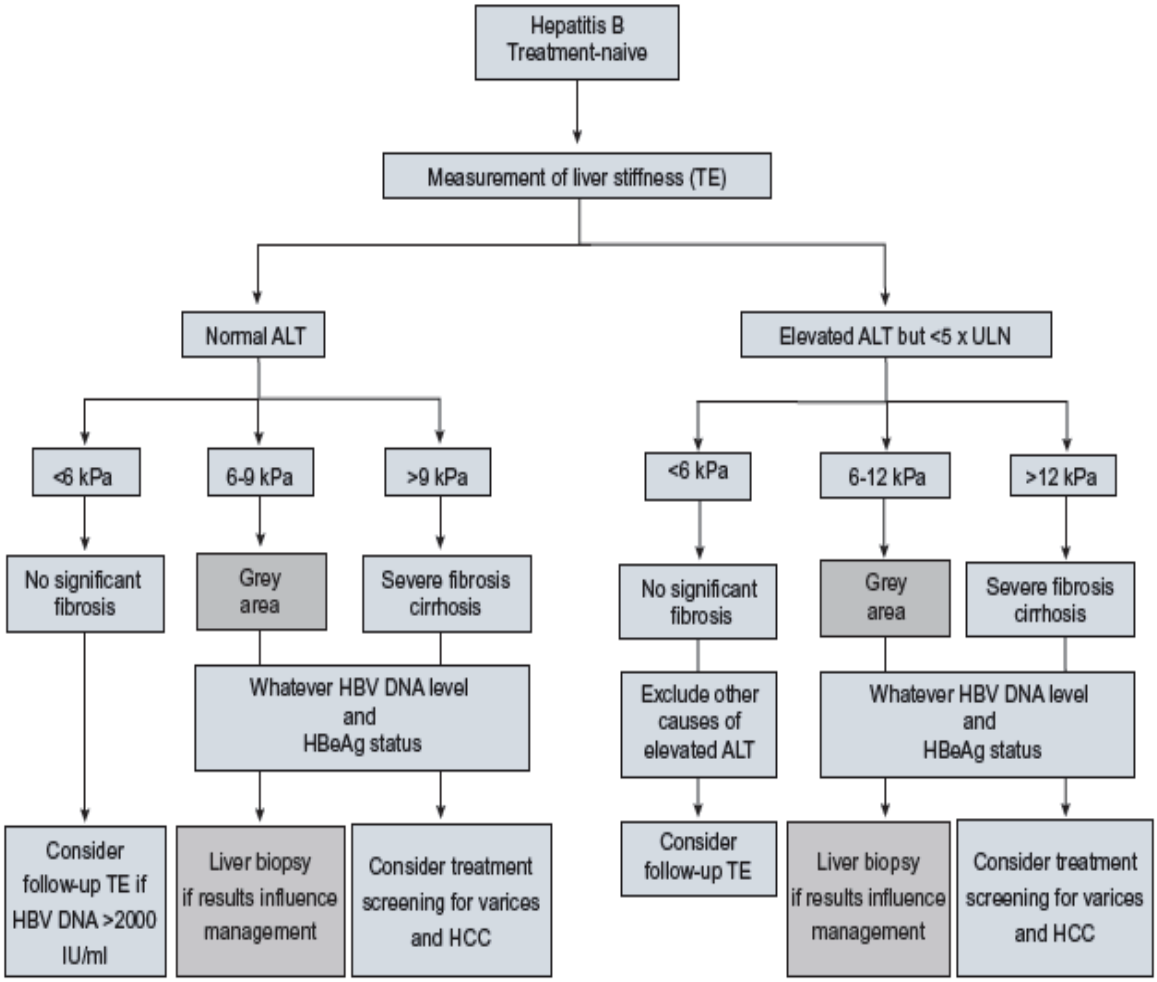

Figure 3: Algorithm in chronic Hepatitis B

PROGNOSTIC VALUE OF NON-INVASIVE TESTS

Shear-wave elastography and serum markers have shown good results in several studies in detecting the presence or bleeding of oesophageal varices by associating elastographic measurement, spleen size and platelet count. Recently it has been shown that splenic stiffness measured by shear-wave elastography has shown a better association with hepatic venous pressure, varicose veins and varicose veins and bleeding [123-124].

Several studies have shown an increased risk of developing hepatocellular carcinoma (HCC) in patients with chronic viral hepatitis with high Fibroscan^{TM} values. A recent study with 1,555 patients with chronic hepatitis B showed that Fibroscan^{TM} score improved the diagnosis of HCC.

Using a cut-off value of 11, Fibroscan™ was able to exclude HCC development at 5 years with a high predictive value of 99-100% negative [125].

In a prospective study involving 1,457 patients with chronic hepatitis C, all patients underwent on the same day liver biopsy, Fibroscan™ measurement and FibroTest™, with FIB-4 and APRI serum markers at zero time and during a five-year follow-up. Patients with METAVIR score F3/F4 had a lower five-year survival rate compared to METAVIR F0/F2 patients. Similar results were obtained using Fibroscan™: patients with Fibroscan™ values <9 and greater than 9.5 kPa had a 5 year survival rate of 77% and 96%, respectively. Patients with FibroTest™ values greater than 0.95 kPa had a five-year survival rate of 0%, while patients with FibroTest™ values below 0.75 kPa had a survival rate of 97%.

Comparable results were obtained in a study that combined Fibroscan™ and FibroTest™ to evaluate five-year survival in patients with chronic Hepatitis B [126-127].

PORTAL HYPERTENSION

Portal hypertension is haemodynamically defined by an increase in the venous pressure gradient across the liver, calculated from its inflow through the portal vein versus its outflow through the hepatic veins. An increase in resistance to portal blood flow is the initial factor that leads to a rise in portal pressure. This resistance can be located at any point in the liver circulation, i.e. at the prehepatic, intrahepatic or post-hepatic level. In the Western world, 90% of cases of PH are due to advanced chronic liver disease (ACLD) or cirrhosis, which cause structural damage through fibrogenesis, parenchymal extinction and regeneration. PH then develops at the intrahepatic sinusoidal site. Other less common causes include vascular liver diseases, such as extrahepatic portal vein obstruction, thrombosis of the hepatic veins (Budd-Chiari syndrome, BCS) and idiopathic PH. Sinusoidal PH in patients with cirrhosis can be reliably and safely evaluated by measuring the hepatic venous pressure gradient (HVPG) via hepatic vein catheterization. An HVPG of up to 5 mmHg is considered normal; subclinical PH is defined by an HVPG of 6–9 mmHg; and

an HVPGP10 mmHg represents the 'clinically significant' PH threshold.4 When HVPG reaches 10 mmHg or above, PH can become symptomatic as patients can develop gastroesophageal varices and hyperdynamic circulation, increasing their risk of clinical decompensation. Upper gastrointestinal endoscopy is the best method to determine the presence of oesophageal and gastric varices, and allows the identification of additional signs used to stratify bleeding risk.

Liver stiffness measurement (LSM) accurately reflects liver fibrosis in CLD.17 In patients with CLD, fibrosis is the major component of increased intrahepatic vascular resistance leading to PH (as discussed above). Therefore, LSM has been studied as a possible surrogate for PH. The spleen undergoes parenchymal remodelling in patients with PH. This is partly attributable to passive congestion and increased arterial inflow, and partly because of increased hyperactive splenic lymphoid tissue and enhanced angiogenesis and fibrogenesis, leading to the progressive development of splenomegaly in most patients. Ultrasound studies showed that spleen vascular resistance (estimated by Doppler pulsatility and resistance indexes) is increased in patients with PH, and correlates with PH severity and complications. Spleen stiffness measurement (SSM) by ultrasound elastography could be an accurate non-invasive surrogate for PH, and devoid of the limitations of LSM. Studies comparing LSM and SSM (measured by TE in an adequate left intercostal space using technical conditions similar to those used for LSM) showed that the spleen is substantially stiffer than the liver in both healthy subjects and patients with chronic liver disease.

CONTROLLED ATTENUATION PARAMETER (CAP score)

Since ultrasound propagation is influenced by the presence of fat in the tissue, new software has been developed to quantify steatosis. This parameter is based on the ultrasonic properties of the radiofrequency signals that are retropropagated and acquired by Fibroscan^{TM}. It is called the Controlled Attenuation Parameter (CAP score) and is generated by a process based on vibration-controlled transient elastography (VCTE) [128-129]. The CAP measures the degree of ultrasound

attenuation by hepatic fat at the central frequency of the Fibroscan^{TM} M probe (3.5 MHz). Results are expressed in decibels per metre (dB/m).

Several studies reported that the CAP correlated fairly well with biopsy proven steatosis and significantly differentiated between S0, S1 and S2 patients. However, a significant difference could not be detected in subjects with advanced disease (S2–S3) [130-131].

Cut-off values vary from one study to another, but the cut-off values associated with significant steatosis (33% of hepatocytes) was almost always 250 dB/m. [132].

Another study reported that larger skin capsular distance (SCD), obesity and metabolic syndrome, when measuring CAP, may cause overestimation of steatosis [133-134-135-136-137]. A CAP algorithm for the Fibroscan^{TM} XL probe, specifically designed for the obese population, is being developed [139]. A recent study on 324 patients with biopsy-proven NAFLD found that CAP, directly related to steatosis and obesity, is independently linked to increased liver stiffness (LS) values, especially in patients with lower stages of fibrosis. A higher rate of false-positive LS results for the assessment of fibrosis by TE in patients in the higher CAP tertiles was noticed. The study also proposed a flowchart based on both LS restuls and CAP score [140].

METHODOLOGY

AIMS & OBJECTIVES

1. To correlate liver stiffness assessed by the Philips EPIQ 7TM ultrasound system, Siemens Acuson (ARFI) ultrasound system, and Echosens Fibroscan™ (currently the best-validated technique), and compare the results of these three imaging techniques with histological results in patients suffering from chronic liver disease with different aetiologies.

2. To determine cut-off values of the liver stiffness (LS) measurements that correlate with the histological fibrosis stage.

3. To detect variations in liver stiffness (LS) measurements correlated with different parameters:

- diagnostic blood tests
- blood pressure
- anthropometric parameters: body mass index (BMI)

4. To correlate CAP score with the histological results of liver biopsy.

STUDY DESIGN

This is an imaging study to compare the results of three imaging techniques (Philips Shear Wave Ultrasound, Siemens Acuson ARFI and Echosens Fibroscan™) with the clinical diagnostic results of liver biopsies.

100 patients were studied using the Philips Ultrasound System, Siemens ARFI Acuson and Fibroscan™ immediately prior to the liver biopsy.

INCLUSION CRITERIA:

- Able and willing to provide written informed consent;
- Aged between 18 and 75;
- Chronic liver disease;

- About to undergo a liver biopsy as part of standard routine clinical care, or if a liver biopsy has already recently been performed, is willing to attend for a specific research visit for the three scans;
- Willing to consent to medical notes and diagnostic test results being reviewed, captured, and recorded by the clinical research study team.

EXCLUSION CRITERIA:

- Unable or unwilling to give written informed consent;
- Aged under 18 or over 75;
- No evidence of liver disease;
- Pregnancy;
- Patients with pacemakers fitted.

STUDY PROCEDURES

Ethical Approval

The study was performed in accordance with the principles of the Declaration of Helsinki and its appendices and with local and national laws. Project-specific ethical approval was successfully obtained on 3 December 2015 from the London City & East NRES Committee (REC reference 15/EE/0420). Full local Trust R&D approval was given on 3 March 2016 (Joint Research Compliance Office Reference N° 187875). This study was adopted as an NIHR CRN Portfolio study on 7 March 2016. Written informed consent was obtained from all patients.

ElastPQ

The Philips system EPIQ 7^{TM} uses the C5- I Pure Waves transducer. Results can be displayed in m/s or in kPa. Fail-safe mode reduces false reading. The maximum penetration depth of ElastPQ was 8 cm and the region of interest (ROI) size measurement was depth dependent with 0.5 cm-1.5 cm at the depth of 4 cm. The ROI measurement and quantitative value of liver stiffness was displayed over a B-mode ultrasound image.

Home / Faculty of Medicine / Departments /
Department of Surgery and Cancer / Research /
Digestive Diseases / Clinical trials

Clinical trials

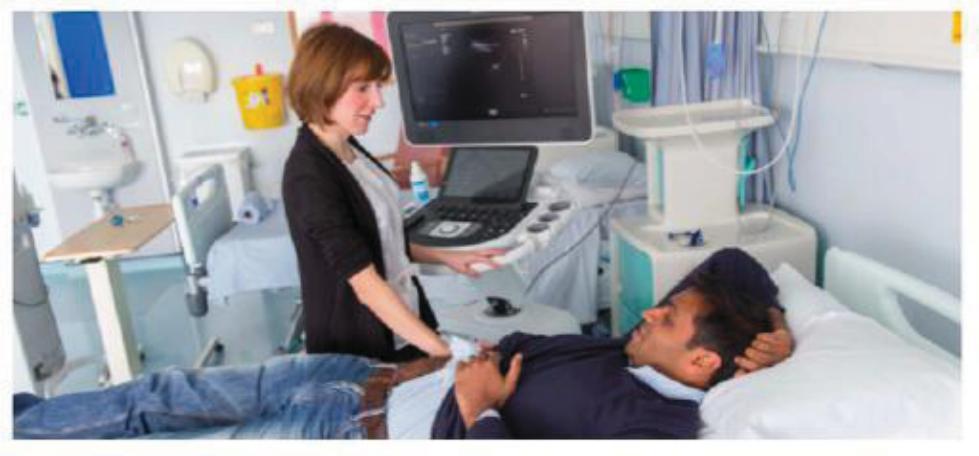

Figure 4: Philips EPIQ 7^{TM}

Patients

Each patient was placed supine with right arm raised behind his/her head and remained still during the procedure. Patients were fasted for up to 6 hours. 10 measurements were taken on the right lobe of the liver, 10 on the left lobe of the liver, 10 on the spleen and a median value calculated for every set of measurements.

Breathing phase

During a normal respiratory phase the participants were invited to hold their breath for a few seconds during the measurements so as to minimise breathing motion while avoiding deep inspiration or expiration. Elast PQ measurements were performed 10 times on the right lobe, 10 times in the left lobe and 10 times in the spleen.

Liver location

10 measurements were taken on the right lobe of the liver, and a median value calculated. On the right lobe of the liver the measurements were taken in approximately the same area where the biopsy was to be performed, an area where the liver tissue was at least 6 cm thick and free of large blood vessels. A measurement depth of 2 cm below the liver capsule was chosen to standardise the examination.

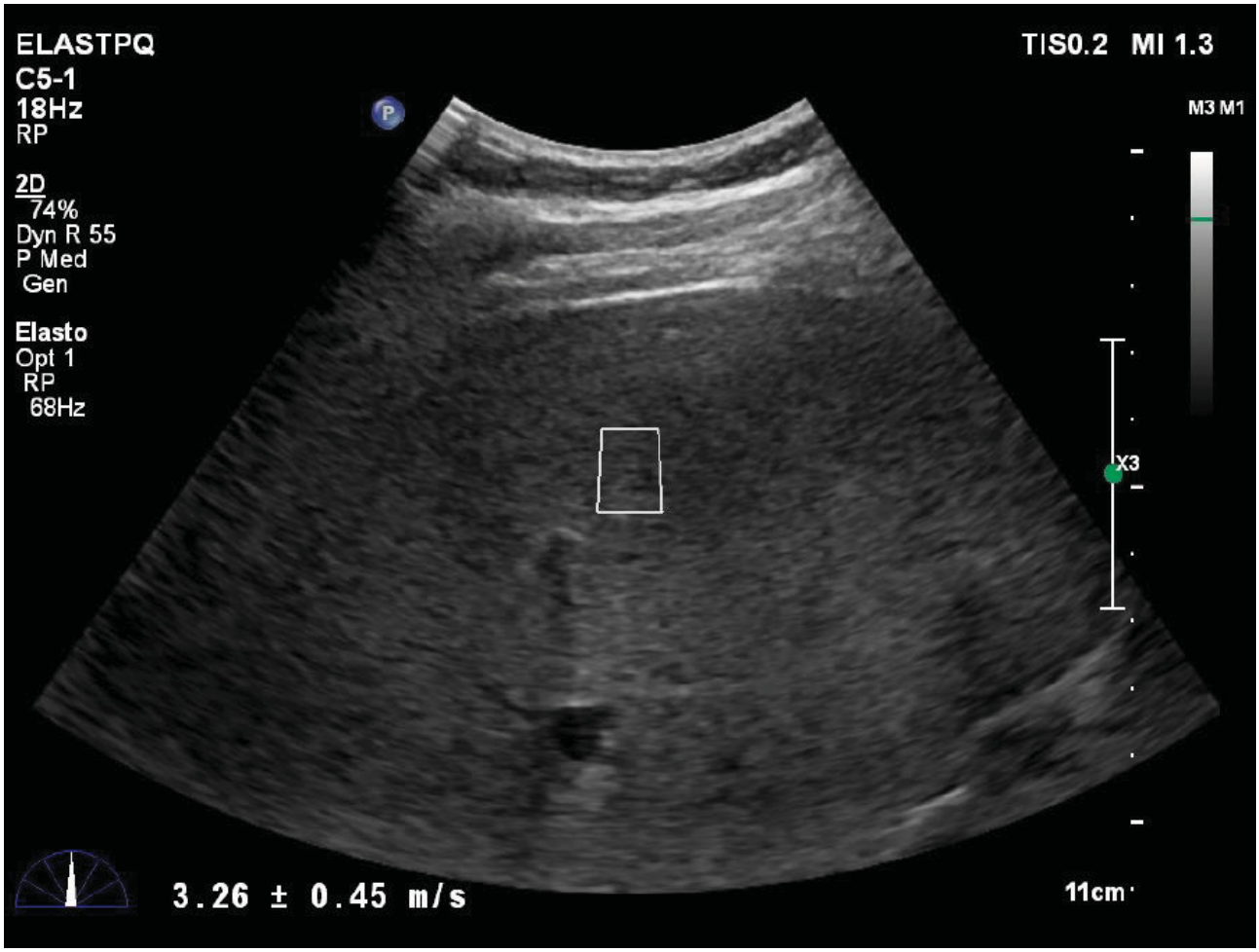

Figure 5: Region of interest in shear-wave elastography measurement

Probe position

Scans of the right lobe of the liver were obtained through an intercostal approach and measurements were taken on the same segment as the liver biopsy. Elast PQ measurements were performed 10 times on the right lobe, 10 times on the left lobe and 10 times on the spleen.

Measurement results

The results are expressed in m/s and kPa. The median of 10 acquisitions was calculated. The 10 measurements were taken in order to obtain the lowest IQR/M.

Virtual Touch HD Tissue

Acoustic Radiation Force Impulse imaging (Virtual Touch Tissue Quantification, Siemens ACUSON S2000, Siemens Medical Solutions, Mountain View, CA, USA) involves targeting an anatomic region to be interrogated for elastic properties with a region of interest (ROI) cursor while performing real-time B-mode imaging. Tissue at the ROI is mechanically excited using short-duration acoustic pulses to generate localised tissue displacements in it. The displacements result in shear-wave propagation away from the region of excitation and are tracked using ultrasonic, correlation-based methods. The shear velocity increases with fibrosis severity and is estimated in the central window 5 mm axial by 4 mm wide, within a region of interest graphically displayed with a size of 1 cm axial by 6 mm width [132].

Patients

Each patient was placed supine with right arm raised behind his/her head and remained still during the procedure. Patients had fasted for up to 6 hours. 10 measurements were taken on the right lobe of the liver, 10 on the left lobe and 10 on the spleen and the median value calculated for every set of measurements.

Breathing phase

During a normal respiratory phase the participants were invited to hold their breath for a few seconds during the measurements. Virtual Touch measurements were performed 10 times on the right lobe of the liver, 10 on the left lobe and 10 on the spleen.

Probe position

Scans on the right lobe of the liver were obtained through an intercostal approach and measurements were taken in the same segment as for the liver biopsy. Virtual Touch measurements were performed 10 times on the right lobe, 10 on the left lobe and 10 on the spleen.

Liver location

10 measurements were taken on the right lobe of the liver and a median value calculated. They were taken in approximately the same area as that where the biopsy was to be performed, an area where the liver tissue was at least 6 cm thick and free of large blood vessels. A measurement depth of 2 cm below the liver capsule was chosen to standardise the examination.

Measurement results

Results are expressed in m/s then converted into kPa using the formula $3*(\text{median in m/s})^2$. The 10 measurements were taken in order to obtain the lowest IQR/M.

Fibroscan™

TE provides only a 1D line and an M-mode image to localise the measurement site.

Patients

Each patient was placed supine with right arm raised behind his/her head and remained still during the procedure. With the probe over the liver region, readings were attempted until 10 valid measurements were obtained.

Probe position

All studies were started with an M+ probe, with an XL+ probe for rescue only when prompted by the automatic probe selection tool. In rare instances, where the machine's recommendation fluctuated between M+ and XL+ probes, the study coordinator was instructed to choose the XL+ probe.

Measurement results

Only results with 10 valid shots and IQR/ median liver stiffness ratio <30% were included.

CAP score

CAP was computed only when the associated liver stiffness measurement was valid and using the same signals as the one used to measure liver stiffness. Therefore, both stiffness and CAP were obtained simultaneously and in the same volume of liver parenchyma (namely between 25 and 65 mm). The final CAP value was the median of individual CAP values and was expressed in dB/m.

Liver biopsy

Liver biopsy was performed by the operator using an 18-gauge trucut needle (Bioprince Argon Medical devices INC) with ultrasound-guided approach. A minimum 20 mm long biopsy specimen was required.

Histological assessment

A minimum 20 mm long biopsy specimen or the presence of at least 10 complete portal tracts was required.

Core biopsy samples were placed in 10% formaldehyde solution and sent to the local Histopathology Department at St Mary's Hospital.

Two expert pathologists, who were blinded to the CAP results and liver stiffness measurement, analysed the liver biopsy (19).

Liver biopsy specimens were formalin-fixed and paraffin-embedded. 4-mm thick sections were stained with haematoxylin-eosin-safran, Masson's trichrome stain for collagen, Perl's stain for iron and Gordon & Sweets stain for reticulin. Liver fibrosis stage and necroinflammatory activity grade were evaluated according to the Metavir or NAS score depending on the cause of disease. Steatosis was categorised by visual assessment steatosis and was defined according to the number of affected hepatocytes: S1 (5–33%, "mild"), S2 (33–66%, "moderate"), S3 (66%, "severe").

Blood samples

Blood sample analysis was carried out at St Mary's Hospital laboratory.

Statistical Methods

Statistical analysis was performed using SPSS, Version 24.0 (IBM Statistics). Spearman's rank correlation coefficient was used to assess the correlation between TE and Elast PQ. Area under receiver operating characteristic (AUROC) curves were calculated for Elast PQ to identify discriminating cut-offs for various stages of liver fibrosis.

RESULTS

This was a single-centre, cross-sectional study. 110 consecutive patients with liver disease who had been referred for a liver biopsy were scanned, immediately prior to their liver biopsy, using the Philips ultrasound system, Siemens Acuson S2000 ARFI ultrasound system and Echosens Fibroscan^{TM}. Liver biopsy was performed on the same day as the pSWE and TE measurements, as day-case procedures. Tests were performed in the morning after an overnight fast. The patients' characteristics, epidemiological data and biochemical test results were recorded.

Between March 2016 and December a total of 126 consecutive patients fulfilled the inclusion criteria. Among them, 9 were excluded because liver biopsy was considered unsuitable for staging. Finally, 110 patients were considered for subsequent analysis. No side-effect was observed. Patients' characteristics are indicated in Table 1,2,3 .

Liver stiffness measurements were not obtained in 2 patients by TE due to ascites. Reliable measurements by Fibroscan^{TM} were obtained by the M probe in 66 patients and by the XL probe in 20 patients. The overall median values of liver stiffness for fibrosis stages and standard deviation of Fibroscan^{TM}, Elast PQ and Virtual Touch are illustrated in Table 3.

A direct, strong correlation was observed between LS values assessed by TE elastography by Elast PQ and Virtual Touch ($p < 0.0001$) and Metavir score.

The AUROCs (Area Under the Received Curves) were calculated considering the liver biopsy as the reference method.

Areas under the Curve (AUC) are: TE 0.829; Elast PQ^{TM} 0.804; VTQ 0.696 for no or mild fibrosis (F0-F1 n=51) and TE 0.946; Elast PQ^{TM} 0.866; VTQ 0.852 for cirrhosis (F4, n= 15 positives).

The mean optimal cut-off for no or mild fibrosis F0-F1 (n=51) are 8.15 kPa for TE (sensitivity 0.76 and specificity 0.80); 7.15 KPa (sensitivity 0.72; specificity 0.80) for ElastPQ^{TM} and 8.2 KPa (sensitivity 0.70 and specificity 0.60) for VTQ. The mean optimal cut-off for cirrhosis F=4 (n=13)

are 15.1 kPa for TE (sensitivity was 0.92 and specificity 0.92); 10.80 KPa (sensitivity 0.84; specificity 0.87) for Elast PQ^{TM} and 11.82 KPa (sensitivity 0.84 and specificity 0.71) for VTQ.

Mean value for Elast PQ^{TM} in the left lobe are higher to those obtained from the right lobe of the liver (Right 8.76 kPa; Left 9.95 kPa) but this is not statistically significant (p=0.105).

The diagnostic accuracy (AUROC) of measures taken on the left lobe are: Elast PQ^{TM} 0.728; VTQ 0.661 for no or mild fibrosis (F0-F1 n=52) and Elast PQ^{TM} 0.796; VTQ 0.773 for cirrhosis (F4, n= 14 positives).

The mean optimal cut-off for no or mild fibrosis F0-F1 (n=52) measured in the left lobe are: 8.3 KPa (sensitivity 0.67; specificity 0.69) for ElastPQ^{TM} and 8.6 KPa (sensitivity 0.63 and specificity 0.57) for VTQ. The mean optimal cut-off for cirrhosis F=4 (n=13) measured on the left lobe of the liver are: 10.18 KPa (sensitivity 0.71; specificity 0.71) for Elast PQ^{TM} and 11.82 KPa (sensitivity 0.71 and specificity 0.76) for VTQ.

Bland-Altman plot shows the agreement betweek Elast PQ^{TM} measurements taken on the right and left lobe of the liver.

All the 3 techniques correlate with histological score of liver fibrosis (METAVIR score). Correlation with serum aminotransferase level shows a statistical significance for TE and Elast PQ^{TM} (r Elast PQ^{TM} 0.253; TE 0.273). Elast PQ^{TM} and Virtual Touch, but not TE, showed statistically significative correlation with lobular activity (Elast PQ^{TM} r 0.26; VTQ 0.26). There is no correlation in all the 3 techniques with histological presence of steatosis and body mass index (BMI).

A linear regression analysis shows correlation between Elast PQ^{TM} measurements and interquartile range (IQR) (r^2 0.50, p 0.002) and transaminases level (r^2 0.064, p 0.002) and between VTQ measurements and IQR (r^2 0.507, p 0.001).

Positive correlation with both steatosis and ballooning on liver biopsy shows a statistical significance for CAP score (r Steatosis 0.558; Ballooning 0.473). CAP score doesn't show statistically significative correlations with BMI and lobular activity (r 0.057; r 0.190 respectively).

Receiver operating characteristic (ROC) curves of steatosis and ballooning measured by CAP score show that CAP score is more accurate in the diagnosis of ballooning (AUROC 0.822) than steatosis (AUROC 0.782).

Comparisons of spleen stiffness (SS) by Elast PQ in the group of patients with HIV and NCPH (n=11), in patients with HIV but no NCPH (n=11), in the subgroup of patients with cirrhosis and non portal hypertension (n= 15) and in patients with no fibrosis (F0, n 15), shows statistically higher values (p 0.01) in patient with NCPH compared to spleen stiffness in patients with HIV without NCPH and in patients with no fibrosis (F0). SS values are also higher but not statistically significative (p 0.060) compared to SS measurements in patients with cirrhosis.

DISCUSSION

Liver biopsy is still considered the gold standard for the evaluation of chronic diffuse liver diseases. However, liver biopsy is an invasive procedure, and its complications occur in 0.6–5% of patients. In recent years, shear-wave-based ultrasound elastography has begun to play an increasingly important role in the assessment of liver stiffness. In this study, we correlated liver stiffness assessed by the Philips EPIQ 7^{TM} Ultrasound System, Siemens Acuson (ARFI) ultrasound system and Echosens Fibroscan^{TM} (currently the best-validated technique), and compared the results of these three imaging techniques with histological results in 87 patients suffering from liver disease with different aetiologies. The results of our study showed that Elast PQ gave a good performance compared with TE and that the cut-off values for TE were 8.07 kPa for the diagnosis of significant fibrosis (fibrosis F1-F3) and 10.35 kPa for the diagnosis of cirrhosis (fibrosis F4). The best liver stiffness cut-offs identified by the ROC curves able to maximise the accuracy of Elast PQ were 6.62 kPa for the diagnosis of significant fibrosis (fibrosis F1-F3) and 8.09 kPa for the diagnosis of cirrhosis (fibrosis F4). These results are consistent with previous studies in the literature.

The CAP score showed significant correlation with two histological components of NASH, steatosis and ballooning, but not for lobular activity. This result could be related to an underestimation of steatosis in the histological results. Tissue sample lengths are usually 20 mm and could underestimate the percentage of steatosis that is often more present in zone 3, while the CAP score, having a more widely-explored volume, could give a better assessment of steatosis.

Elevated spleen stiffness is observed in HIV patients with NCPH and can be quantified easily using shear wave elastography. Further evaluation for longitudinal monitoring of patients with portal hypertension should be considered.

The multiple aetiologies of liver disease are a limitation of this study, but it reflects the different liver disease aetiologies that have undergone a liver biopsy as a standard of care. Considering the

fact that fewer patients undergo a liver biopsy nowadays, a sample size of 110 patients with liver biopsy is important to detect the reliability of non-invasive techniques.

Further studies are needed in order to better understand non-invasive assessment of liver fibrosis and steatosis.

TABLES OF RESULTS

	FREQUENCIES	MEAN
M	64	
F	46	
Age		47.98+-13.8
Total	110	

Table 1 Patients' Profile

	AETIOLOGY
NAFLD	**47**
HBV	**22**
NAFLD/HIV	**7**
AIH	**10**
PSC	**4**
DILI	**6**
OTHER	**14**

Table 2 Patients' profile. AIH: autoimmune hepatitis; NASH: non alcoholic steatohepatitis; HBV: chronic hepatitis B; HCV chronic hepatitis C; ALD: alcohol liver disease; PSC: primary sclerosing cholangitis; DILI: drug induced liver disease.

METAVIR	
0	16
1	40
2	20
3	19
4	15

Table 3: Histologica features according METAVIR score.

	Fibroscan	IQR	Elast PQ	IQR	Virtual Touch	IQR
Mean	10.75	1.4	8.90	4.61	11.03	7.22
Median	8.0	0.85	6.86	2.91	9.19	5.15
SD	9.50	2.54	6.66	5.82	7.30	6.9

Table 4 Mean and median value measurements on the right lobe for FIbroscan Elast PQ and Virtual Touch

	Elast PQ L	IQR	Virtual Touch L	IQR
Mean	9.95	6.93	10.74	7.31
Median	8.27	3.98	8.78	4.86
SD	7.98	10.04	6.53	5.82

Table 5 Mean and median value measurements on the left lobe for FIbroscan Elast PQ and Virtual Touch

	Spleen Elast Q	IQR	Spleen VTQ	IQR
Mean	23.97	14.61	21.45	12.56
Median	19.71	9.06	20.43	10.64
SD	29.35	25.98	7.38	8.51

Table 6 Mean and median value measurements of the spleen for Elast PQ and Virtual Touch

	Metavis	ElastPQ	VTQ	Fibroscan	ALT	AST	Platelet
Metavir	1	0.480 p <0.001 R^2 0.230	0.413 p <0.001 R^2 0.17	0.476 p <0.001 R^2 0.22	-0.093 p 0.33	-0.020 p 0.88	-0.156 p 0.104
ElastPQ	0.480 p <0.001	1	0.432 p <0.001	0.590 p <0.001	0.253 p 0.008	0.342 p <0.001	-0.080 p 0.404
VTQ	0.413 p <0.001	0.432 p <0.001	1	0.471 p <0.001	0.036 p 0.711	0.068 p 109	-0.2235 p 0.014
Fibroscan	0.476 p <0.001	0.590 p <0.001	0.471 p <0.001	1	0.273 p 0.004	0.348 p <0.001	-0.245 p 0.011

Table 7 Pearson Correlation

	AGE	BMI	DISTANCE SKIN/CAPSULE
METAVIR	0.300 p 0.001	0.219 p 0.021	-0.053 p 0.582
ELAST PQ	0.184 p 0.055	0.131 p 0.173	-0.056 p 0.559
VTQ	0.405 p <0.001	0.096 p 0.319	-0.089 p 0.358
FIBROSCAN	0.271 p 0.005	0.159 p 0.101	-0.054 p 0.584

Table 8 Pearson Correlation

	STEATOSIS	BALLOONING	LOBULAR ACTIVITY
ELAST PQ	-0.098 0.309	0.092 0.339	0.262 0.006
VTQ	0.030 0.758	0.186 0.053	0.266 0.005
FIBROSCAN	-0.082 0.400	0.048 0.622	0.136 0.164

Table 9 Pearson Correlation

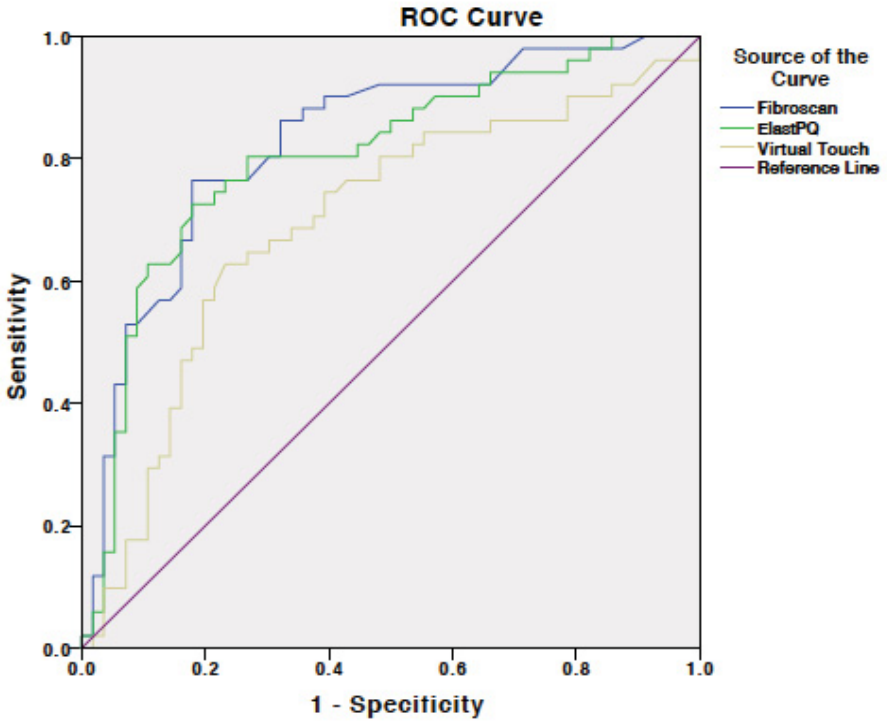

Figure 1 Areas under the Curve (AUC): TE, Elast PQ™ ,VTQ for F0-F1

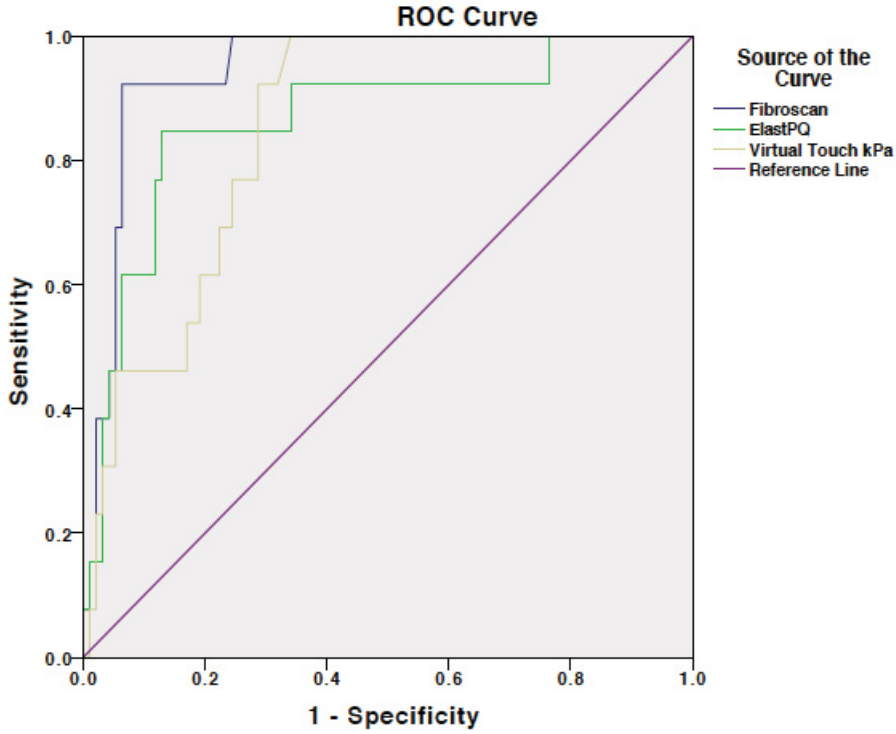

Figure 2 Areas under the Curve (AUC): TE, Elast PQ™, VTQ for F4

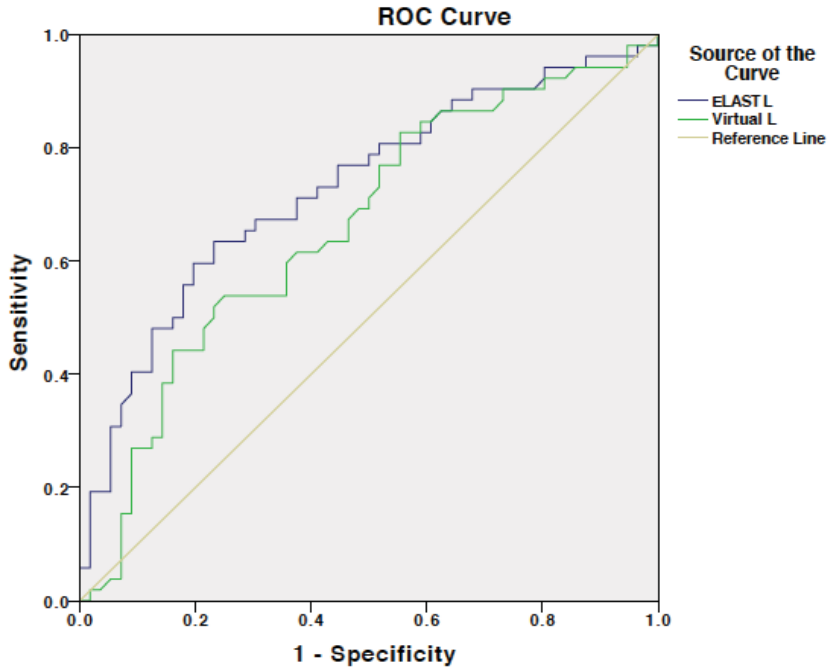

Figure 3 Areas under the Curve (AUC) measured on the left lobe: Elast PQ™, VTQ for diagnosis of fibrosis F0-F1

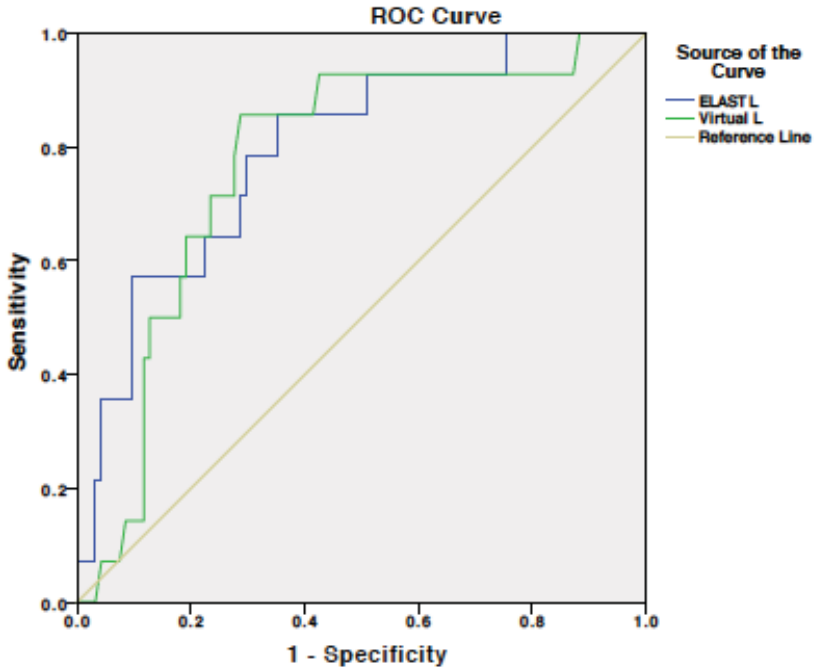

Figure 4 Areas under the Curve (AUC) measured on the left lobe: Elast PQ™, VTQ for diagnosis of cirrhosis (F4)

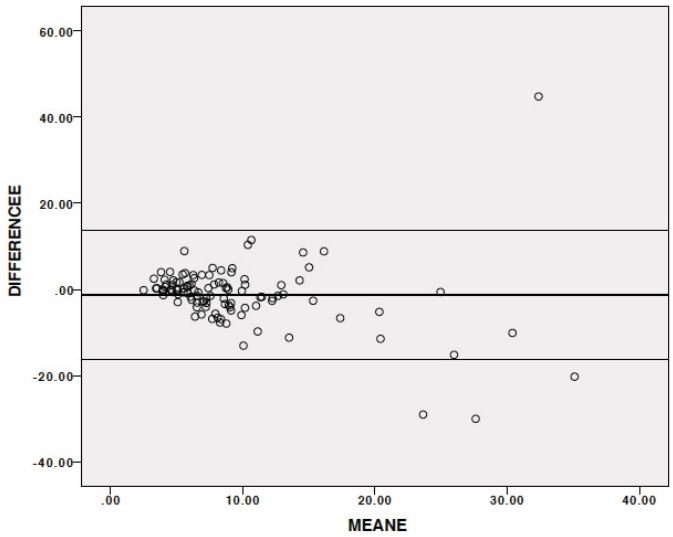

Figure 5 Bland-Altman shows agreement between measurements taken on the right and left lobe of the liver by Elast PQ

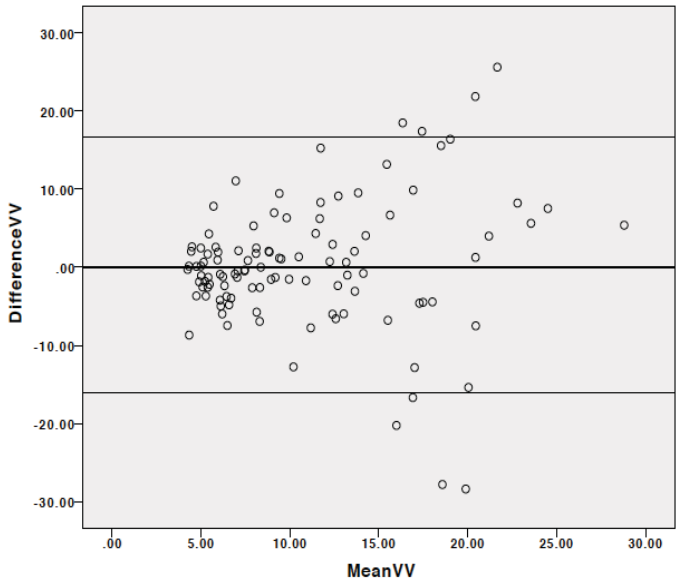

Figure 6 Bland-Altman shows agreement between measurements taken on the right and left lobe of the liver by Virtual Touch

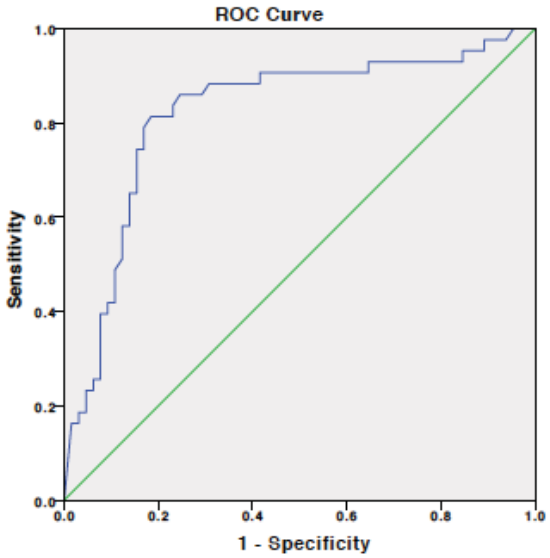

Figure 7 Area under the Curve (AUC): CAP score for diagnosis of Ballooning

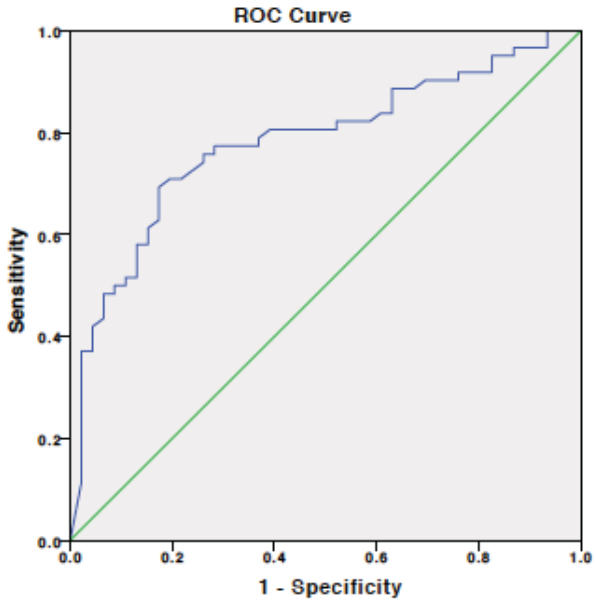

Figure 8 Area under the Curve: CAP score for diagnosis of Steatosis

SS

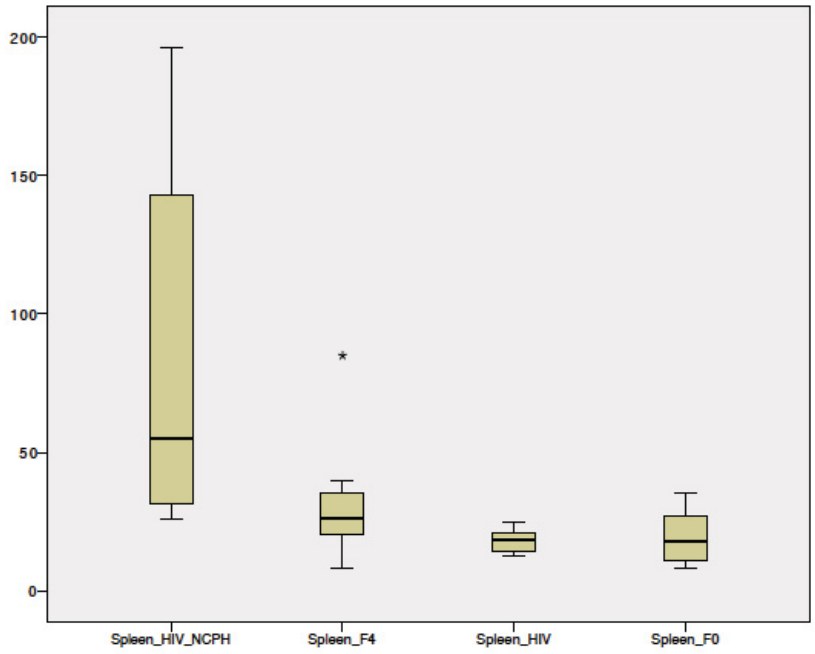

Figura 9 Distribution of spleen stiffness median values measured by Elast PQ™ among patients with NCPH, cirrhotic patients and healthy controls. Spleen stiffness measurements in patients with HIV and non cirrhotic (NCPH); spleen stiffness measurement in patients with cirrhosis (F4); spleen stiffness measurements in patients with HIV and spleen stiffness measurements in patients with fibrosis F0.

REFERENCES

[1] Bataller R, Brenner DA. Liver fibrosis. J Clin Invest 2005;115:209-218. Erratum in: J Clin Invest 2005;115:1100.

[2] Cadranel JF, Rufat P, Degos F. Practices of liver biopsy in France: results of a prospective nationwide survey. For the Group of Epidemiology of the French Association for the Study of the Liver (AFEF). Hepatology 2000;32: 477-481.

[3] Regev A, Berho M, Jeffers LJ, Milikowski C, Molina EG, Pyrsopoulos NT, et al. Sampling error and intraobserver variation in liver biopsy in patients with chronic HCV infection. Am J Gastroenterol 2002;97: 2614-2618.

[4] Manning DS, Afdhal NH. Diagnosis and quantitation of fibrosis. Gastroenterology 2008; 134:1670-1681.

[5] Aubé C, Oberti F, Korali N, Namour MA, Loisel D, Tanguy JY, et al. Ultrasonographic diagnosis of hepatic fibrosis or cirrhosis. J Hepatol 1999;30:472-478.

[6] de Lédinghen V, Vergniol J. Transient elastography for the diagnosis of liver fibrosis. Expert Rev Med Devices 2010;7:811-823.

[7] Friedrich-Rust M, Wunder K, Kriener S, Sotoudeh F, Richter S, Bojunga J, et al. Liver fibrosis in viral hepatitis: noninvasive assessment with acoustic radiation force impulse imaging versus transient elastography. Radiology 2009; 252:595-604.

[8] Friedman SL. Liver fibrosis - from bench to bedside. J Hepatol 2003; 38(S1):S38–S53.

[9] Friedman SL. Gastroenterology 134 2008;1655–1669.

[10] Parola M, Marra F, Pinzani M. Mol. Aspects Med. 29 2008; 58–66.

[11] Dranoff JA, Wells RG. Hepatology 51 2010; 1438–1444.

[12] Forbes SJ, Parola M. Best Pract. Res. Clin. Gastroenterol. 25 2011; 207–218.

[13] Zhang DY, Friedman SL. Hepatology 56 2012; 769–775.

[14] Geerts A. History, heterogeneity, developmental biology and functions of quiescent hepatic stellate cells. Semin Liver Dis 2001; 21: 311–335.

[15] Davis GL, Albright JE, Cook SF et al. Projecting future complications of chronic hepatitis C in the United States. Liver Transpl 2003; 9: 331–338.

[16] Ramadori G, Zohrens G, Manns M et al. Serum hyaluronate and type III procollagen aminoterminal propeptide concentration in chronic liver disease. Relationship to cirrhosis and disease activity. Eur J Clin Invest 1991; 21: 323-30.

[17] Takehara T. Hepatocyte-specific disruption of Bcl-xL leads to continuous hepatocyte apoptosis and liver fibrotic responses. Gastroenterology 2004; 127: 1189–1197.

[18] Bataller R, North KE, Brenner DA. Genetic polymorphisms and the progression of liver fibrosis: a critical appraisal. Hepatology 2003; 37: 493–503.

[19] Oben JA. Hepatic fibrogenesis requie sympathetic neurotransmitters. Gut 2004; 53: 438-445.

[20] Ueberham E. Conditional tetracyclineregulated expression of TGF-beta1 in liver of transgenic mice leads to reversible intermediary fibrosis. Hepatology 2003; 37: 1067–1078.

[21] Pinzani M. Liver fibrosis. Springer Semin Immunopathol 1999; 21: 475–490.

[22] Arthur MJ. Fibrogenesis II. Metalloproteinases and their inhibitors in liver fibrosis. Am J Physiol Gastrointest Liver Physiol 2000; 279: G245–G249.

[23] Marra F. Hepatic stellate cells and the regulation of liver inflammation. J Hepatol 1999; 31: 1120–1130.

[24] Lindquist JN, Marzluff WF, Stefanovic B. Fibrogenesis. III. Posttranscriptional regulation of type I collagen. Am J Physiol Gastrointest Liver Physiol 2000; 279: G471–G476.

[25] Lindquist JN, Parsons CJ, Stefanovic B et al. Regulation of alpha1(I) collagen messenger RNA decay by interactions with alphaCP at the 3′-untranslated region. J Biol Chem 2004; 279: 23822–23829.

[26] Kinnman N, Housset C. Peribiliary myofibroblasts in biliary type liver fibrosis. Front Biosci 2002; 7: d496–d503.

[27] Suskind DL, Muench MO. Searching for common stem cells of the hepatic and hematopoietic systems in the human fetal liver: CD34+ cytokeratin 7/8+ cells express markers for stellate cells. J Hepatol 2004; 40: 261–268.

[28] Canbay A, Friedman S, Gores GJ. Apoptosis: the nexus of liver injury and fibrosis. Hepatology 2004; 39: 273–278.

[29] Casini A. Neutrophil-derived superoxide anion induces lipid peroxidation and stimulates collagen synthesis in human hepatic stellate cells: role of nitric oxide. Hepatology 1997; 25: 361–367.

[30] Vinas O. Human hepatic stellate cells show features of antigen-presenting cells and stimulate lymphocyte proliferation. Hepatology 2003; 38: 919–929.

[31] Shi Z, Wakil AE, Rockey DC. Strainspecific differences in mouse hepatic wound healing are mediated by divergent T helper cytokine responses. Proc Natl Acad Sci 1997; 94: 10663–10668.

[32] Naito M, Hasegawa G, Ebe Y et al. Differentiation and function of Kupffer cells. Med Electron Microsc 2004; 37: 16–28.

[33] Gressner AM, Weiskirchen R, Breitkopf K et al. Roles of TGF-beta in hepatic fibrosis. Front Biosci 2002; 7: d793–d807.

[34] Schwabe RF, Bataller R, Brenner DA. Human hepatic stellate cells express CCR5 and RANTES to induce proliferation and migration. Am J Physiol Gastrointest Liver Physiol 2003; 285: G949–G958.

[35] Shek FW, Benyon RC. How can transforming growth factor beta be targeted usefully to combat liver fibrosis? Eur J Gastroenterol Hepatol 2004; 16: 123–126.

[36] Olaso E. DDR2 receptor promotes MMP-2–mediated proliferation and invasion by hepatic stellate cells. J Clin Invest 2001; 108: 1369–1378.

[37] Williams EJ. Relaxin inhibits effective collagen deposition by cultured hepatic stellate cells and decreases rat liver fibrosis in vivo. Gut 2001; 49: 577–583.

[38] Paizis G. Up-regulation of components of the renin-angiotensin system in the bile duct-ligated rat liver. Gastroenterology 2002; 123: 1667-1676.

[39] Paizis G. Up-regulation of components of the renin-angiotensin system in the bile duct-ligated rat liver. Gastroenterology 2002; 123: 1667-1676.

[40] Novo E. Cellular and molecular mechanisms in liver fibrogenesis. Archives of Biochemistry and Biophysics 2014; 548: 20-37.

[41] Chen TJ, Liaw YF. The prognostic significance of bridging hepatic necrosis in chronic type B hepatitis: a histopathologic study. Liver 1988; 8: 10-16.

[42] Okuno T, Okanoue T, Takino T et al. Prognostic significance of bridging necrosis in chronic active hepatitis. Gastroenterol Jpn 1983; 18: 577-584.

[43] Brunt E.M. Grading and staging the histopathological lesions of chronic hepatitis: the Knodell histology activity index and beyond. Hepatology 2000; 31: 241-246.

[44] Ishak K[1], Baptista A, Bianchi L, Callea F, De Groote J, Gudat F, Denk H, Desmet V, Korb G, MacSween RN. Histological grading and staging of chronic hepatitis. J Hepatol. 1995 Jun;22(6):696-9.

[45] Bedossa P, Poynard T. An algorithm for the grading of activity in chronic hepatitis C. The METAVIR Cooperative Study Group. Hepatology 1996; 24: 289-293.

[46] Kleiner DE, Brunt EM, Van Natta M, et al. Design and validation of a histological scoring system for nonalcoholic fatty liver disease. Hepatology. 2005;41:1313–1321.

[47] Younossi ZM, Stepanova M, Rafiq N, et al. Pathologic criteria for nonalcoholic steatohepatitis: interprotocol agreement and ability to predict liver-related mortality. Hepatology. 2011;53:1874–1882.

[48] Ekstedt M, Franzen LE, Mathiesen UL, et al. Long-term followup of patients with NAFLD and elevated liver enzymes. Hepatology. 2006;44:865–873.

[49] Campos GM, Bambha K, Vittinghoff E, et al. A clinical scoring system for predicting nonalcoholic steatohepatitis in morbidly obese patients. Hepatology. 2008;47:1916–1923.

[50] Yeh MM, Brunt EM. Pathological features of fatty liver disease. Gastroenterology. 2014;147:754–764.

[51] Sakhuja P. Pathology of alcoholic liver disease, can it be differentiated from nonalcoholic steatohepatitis? World J Gastroenterol. 2014;20:16474–16479.

[52] Guy CD, Suzuki A, Burchette JL, et al. Costaining for keratins 8/18 plus ubiquitin improves detection of hepatocyte injury in nonalcoholic fatty liver disease. Hum Pathol. 2012;43:790–800.

[53] Rockey DC, Caldwell SH, Goodman ZD et al. Liver biopsy. Hepatology 2009; 49: 1017-1044.

[54] Cholongitas E, Senzolo M, Standish R et al. A systematic review of the quality of liver biopsy specimens. Am J Clin Pathol 2006; 125: 710-721.

[55] Pasha T, Gabriel S, Therneau T et al. Cost-effectiveness of ultrasound-guided liver biopsy. Hepatology 1998; 27: 1220-1226.

[56] Younossi ZM, Teran JC, Ganiats TG et al. Ultrasound-guided liver biopsy for parenchymal liver disease: an economic analysis. Dig Dis Sci 1998; 43: 46-50.

[57] Riley TR 3rd. How often does ultrasound marking change the liver biopsy site? Am J Gastroenterol 1999; 94: 3320-3322.

[58] Piccinino F, Sagnelli E, Pasquale G et al. Complications following percutaneous liver biopsy. A multicenter study on 68276 biopsies. J Hepatol 1986; 2: 165-173.

[59] Bravo AA, Shieth SG, Chopra S. Liver biopsy. New Engl J Med 2001; 344(7): 495-499.

[60] Gunneson TJ, Menon KV, Wiesner RH et al. Ultrasound assisted percutaneous liver biopsy performed by a physician assistant. Am J Gastroenterol 2002; 97: 1472-1475.

[61] McGill D, Rakela J, Zinsmeister AR et al. A 21-year experience with major hemorrhage after percutaneous liver biopsy. Gastroenterology 1990; 99: 1396-1400.

[62] Wong JB, Koff RS. Watchful waiting with periodic liver biopsy versus immediate empirical therapy for histologically mild chronic hepatitis C. A cost-effectiveness analysis. Ann Intern Med 2000; 133:665-675.

[63] Regev A, Berho M, Jeffers LJ et al. Sampling error and intraobserver variation in liver biopsy in patients with chronic HCV infection. Am J Gasstroenterol 2002; 97: 2614-2608.

[64] Maharaj B, Maharaj RJ, Leary WP et al. Sampling variability and its influence on the diagnostic yield of percutaneous needle biopsy of the liver. Lancet 1986; 1: 523-525.

[65] Poniachik J, Bernstein De, Reddy KR et al. The role of laparoscopy in the diagnosis of cirrhosis. Gastrointest Endosc 1996; 43: 568-571.

[66] EASL-ALEH Clinical Practice Guidelines: Non-invasive tests for evaluation of liver disease severity and prognosis Journal of Hepatology 2015 vol. 63 j 237–264.

[67] Lin Z. Performance of the aspartate aminotranferase-to-platelet ratio index for the staging of hepatitis C-related fibrosis: an updated meta-analysis. Hepatology 2011; 53: 726-736.

[68] Shaheen AA. Performance of the aspartate aminotransferase-to-platelet ratio index for the prediction of hepatitis C-related fibrosis: a systemic review. Hepatology 2007; 46: 912-921.

[69] Leroy V. Diagnostic accuracy, reproducibility and robustness of fibrosis blood tests in chronic hepatitis C: a meta-analysis with individual data. Clin Biochem 2008; 41: 1368-1376.

[70] Degos F. Diagnostic accuracy of FibroScan and comparison to liver fibrosis biomarkers in chronic viral hepatitis: a multicenter prospective study (the FIBROSTIC study). J Hepatol 2010; 53: 1013-1021.

[71] Berzigotti A, Castera L. Update on ultrasound imaging of liver fibrosis. J Hepatol 2013;59:180–182.

[72] Sumeet K. Asrani. Incorporation of Noninvasive Measures of Liver Fibrosis Into Clinical Practice: Diagnosis and Prognosis Measurement of liver stiffness. Clinical Gastroenterology and Hepatology 2015;13:2190–2204.

[73] Bamber J et al. EFSUMB Guidelines and and Recommendations on the Clinical Use of Ultrasound Elastography. Part 1: Basic Principles and Technology Ultraschall in Med 2013; 34: 169–184.

[74] Sarvazyan AP, Rudenko OV, Swanson SD et al. Shear wave elasticity imaging: a new ultrasonic technology of medical diagnostics. Ultrasound Med Biol 1998; 24: 1419–1435.

[75] Nightingale K, Soo MS, Nightingale R et al. Acoustic radiation force impulseimaging: in vivo demonstration of clinical feasibility. Ultrasound Med Biol 2002; 28: 227–235.

[76] Palmeri ML, Nightingale KR. Acoustic radiation force-based elasticity imaging methods. Interface Focus 2011; 1: 553–564.

[77] Bercoff J, Pernot M, Tanter M et al. Monitoring thermally-induced lesions with supersonic shear imaging. Ultrason Imaging 2004; 26:71–84.

[78] Bercoff J, Tanter M, Fink M. Supersonic shear imaging: a new technique for soft tissue elasticity mapping. IEEE Trans Ultrason Ferroelectr Freq Control 2004; 51: 396–409.

[79] Roulot D, Czernichow S, Le Clesiau H, Costes JL, Vergnaud AC, Beaugrand M. Liver stiffness values in apparently healthy subjects: influence of gender and metabolic syndrome. J Hepatol 2008;48:606–613.

[80] Kim SU, Choi GH, Han WK, Kim BK, Park JY, Kim do Y, et al. What are 'true normal' liver stiffness values using FibroScan: a prospective study in healthy living liver and kidney donors in South Korea. Liver Int 2010;30:268–274.

[81] Fraquelli M, Rigamonti C, Casazza G, Conte D, Donato MF, Ronchi G, et al. Reproducibility of transient elastography in the evaluation of liver fibrosisin patients with chronic liver disease. Gut 2007;56:968–973.

[82] Boursier J, Konate A, Gorea G, Reaud S, Quemener E, Oberti F, et al. Reproducibility of liver stiffness measurement by ultrasonographic elastometry. Clin Gastroenterol Hepatol 2008;6:1263–1269.

[83] Castera L, Foucher J, Bernard PH, Carvalho F, Allaix D, Merrouche W, et al. Pitfalls of liver

[84] stiffness measurement: a 5-year prospective study of 13,369 examinations. Hepatology 2010;51:828–835.

[85] Wong GL, Wong VW, Chim AM, Yiu KK, Chu SH, Li MK, et al. Factors associated with unreliable liver stiffness measurement and its failure with transient elastography in the Chinese population. J Gastroenterol Hepatol 2011;26:300–305.

[86] Lucidarme D, Foucher J, Le Bail B, Vergniol J, Castera L, Duburque C, et al. Factors of accuracy of transient elastography (Fibroscan) for the diagnosis of liver fibrosis in chronic hepatitis C. Hepatology 2009:1083–1089.

[87] Boursier J, Zarski JP, de Ledinghen V, Rousselet MC, Sturm N, Lebail B, et al. Determination of reliability criteria for liver stiffness evaluation by transient elastography. Hepatology 2013;57:1182–1191.

[88] Friedrich-Rust M, Hadji-Hosseini H, Kriener S, Herrmann E, Sircar I, Kau A, et al. Transient elastography with a new probe for obese patients for non-invasive staging of non-alcoholic steatohepatitis. Eur Radiol 2010;20:2390–2396.

[89] de Ledinghen V, Vergniol J, Foucher J, El-Hajbi F, Merrouche W, Rigalleau V. Feasibility of liver transient elastography with FibroScan using a new probe for obese patients. Liver Int 2010;30:1043–1048.

[90] Myers RP, Pomier-Layrargues G, Kirsch R, Pollett A, Duarte-Rojo A, Wong D, et al. Feasibility and diagnostic performance of the FibroScan XL probe for liver stiffness measurement in overweight and obese patients. Hepatology 2012;55:199–208.

[91] Sandrin L, Fourquet B, Hasquenoph JM, Yon S, Fournier C, Mal F, et al. Transient elastography: a new noninvasive method for assessment of hepatic fibrosis. Ultrasound Med Biol 2003;29:1705–1713.

[92] Coco B, Oliveri F, Maina AM, Ciccorossi P, Sacco R, Colombatto P, et al. Transient elastography: a new surrogate marker of liver fibrosis influenced by major changes of transaminases. J Viral Hepat 2007;14:360–369.

[93] Sagir A, Erhardt A, Schmitt M, Haussinger D. Transient elastography is unreliable for detection of cirrhosis in patients with acute liver damage. Hepatology 2007;47:592–595.

[94] Arena U, Vizzutti F, Corti G, Ambu S, Stasi C, Bresci S, et al. Acute viral hepatitis increases liver stiffness values measured by transient elastography. Hepatology 2008;47:380–384.

[95] Millonig G, Reimann FM, Friedrich S, Fonouni H, Mehrabi A, Buchler MW, et al. Extrahepatic cholestasis increases liver stiffness (FibroScan) irrespective of fibrosis. Hepatology 2008;48:1718–1723.

[96] Gaia S, Carenzi S, Barilli AL, Bugianesi E, Smedile A, Brunello F, et al. Reliability of transient elastography for the detection of fibrosis in nonalcoholic fatty liver disease and chronic viral hepatitis. J Hepatol 2011;54:64–71.

[97] Wong VW, Vergniol J, Wong GL, Foucher J, Chan HL, Le Bail B, et al. Diagnosis of fibrosis and cirrhosis using liver stiffness measurement in nonalcoholic fatty liver disease. Hepatology 2010;51:454–462.

[98] Friedrich-Rust M, Ong MF, Martens S et al. Performance of transient elastography for the staging of liver fibrosis: a meta-analysis. Gastroenterology 2008; 134: 960-974.

[99] Castera L, Vergniol J, Foucher J et al. Prospective comparison of transient elastography, Fibrotest, APRI, and liver biopsy for the assessment of fibrosis in chronic hepatitis C. Gastroenterology 2005; 128: 343-350.

[100] Sporea I, Şirli R, Deleanu A, et al. Comparison of the liver stiffness measurement by transient elastography with the liver biopsy. World J Gastroenterol 2008; 14: 6513-6517.

[101] Sporea I, Helge Gilja O, Bota S, Şirli R, Popescu A. Liver Elastography – An Update. Med Ultrason 2013; 15(4): 304-314.

[102] Marcellin P, Ziol M, Bedossa P, et al. Non-invasive assessment of liver fibrosis by stiffness measurement in patients with chronic hepatitis B. Liver Int 2009 ; 29: 242-247.

[103] Sporea I, Şirli R, Deleanu A, et al. Liver stiffness measurements in patients with HBV vs HCV chronic hepatitis: a comparative study. World J Gastroenterol 2010; 16: 4832- 4837.

[104] Cardoso AC, Carvalho-Filho RJ, Stern C, et al. Direct comparison of diagnostic performance of transient elastography in patients with chronic hepatitis B and chronic hepatitis C. Liver Int 2012; 32: 612-621.

[105] Chan HL, Wong GL, Choi PC, et al. Alanine aminotransferase- based algorithms of liver stiffness measurement by transient elastography (Fibroscan) for liver fibrosis in chronic hepatitis B. J Viral Hepatol 2009; 16: 36-44.

[106] Tsochatzis EA, Gurusamy KS, Ntaoula S, et al. Elastography for the diagnosis of severity of fibrosis in chronic liver disease: a meta-analysis of diagnostic accuracy. J Hepatol 2011; 54: 650-659.

[107] Nguyen-Khac E, Chatelain D, Tramier B, et al. Assessment of asymptomatic liver fibrosis in alcoholic patients using Fibroscan: prospective comparison with seven non-invasive laboratory tests. Aliment Pharmacol Ther 2008; 28: 1188- 1198.

[108] Mueller S, Millonig G, Sarovska L, et al. Increased liver stiffness in alcoholic liver disease: differentiating fibrosis from steatohepatitis. World J Gastroenterol 2010; 16: 966- 972.

[109] Carrion JA, Navasa M, Bosch J, Bruguera M, Gilabert R, Forns X. Transient elastography for diagnosis of advanced fibrosis and portal hypertension in patients with hepatitis C recurrence after liver transplantation. Liver Transpl 2006; 12: 1791-1798.

[110] Bolognesi M, Merkel C, Sacerdoti D, Nava V, Gatta A. Role of spleen enlargement in cirrhosis with portal hypertension. Dig Liver Dis 2002; 34: 144-150.

[111] Bureau C, Metivier S, Peron JM, et al. Transient elastography accurately predicts presence of significant portal hypertension in patients with chronic liver disease. Aliment Pharmacol Ther 2008; 27: 1261-1268.

[112] Robic MA, Procopet B, Métivier S, et al. Liver stiffness accuratelypredicts portal hypertension related complications in patients with chronic liver disease: a prospective study. J Hepatol 2011; 55: 1017-1024.

[113] Castera L, Le Bail B, Roudot-Thoraval F, et al. Early detection in routine clinical practice of cirrhosis and oesophageal, varices in chronic hepatitis C: Comparison of transient elastography (FibroScan) with standard laboratory tests and non-invasive scores. J Hepatol 2009; 50: 59-68.

[114] Pritchett S, Cardenas A, Manning D, Curry M, Afdhal NH. The optimal cut-off for predicting large oesophageal varices using transient elastography is disease specific. J Viral Hepat. 2011; 18: e75-e80.

[115] Shi KQ, Fan YC, Pan ZZ, et al. Transient elastography: a meta-analysis of diagnostic accuracy in evaluation of portal hypertension in chronic liver disease. Liver Int 2013; 33: 62-

[116] Friedrich-Rust M, Wunder K, Kriener S, et al. Liver fibrosis in viral hepatitis: noninvasive assessment with acoustic radiation force impulse imaging versus transient elastography. Radiology 2009; 252: 595-604.

[117] Fierbinteanu-Braticevici C, Andronescu D, Usvat R, Cretoiu D, Baicus C, Marinoschi G. Acoustic radiation force imaging for noninvasive staging of liver sonoelastography fibrosis. World J Gastroenterol 2009; 15: 5525-5532.

[118] Lupşor M, Badea R, Stefanescu H, et al. Performance of a new elastographic method (ARFI technology) compared to unidimensional transient elastography in the noninvasive assessment of chronic hepatitis C. Preliminary results. J Gastrointest Liver Disease 2009; 3: 303-311.

[119] Bavu E, Gennisson JL, Couade M, et al. Noninvasive in vivo liver fibrosis evaluation using supersonic shear imaging: a clinical study on 113 hepatitis C virus patients. Ultrasound Med Biol 2011; 37: 1361-1373.

[120] Ferraioli G, Tinelli C, Dal Bello, et al. Performance of Real- Time Elastography in the Assessment of Liver Fibrosis in Chronic Hepatitis. Hepatology 2011; 4 (Suppl. 1): 816A.

[121] Castera L, Sebastiani G, Le Bail B, et al. Prospective comparison of two algorithms combining non-invasive methods for staging liver fibrosis in chronic hepatitis C. J Hepatol 2010;52:191-198.

[122] Chan HL1, Wong GL, Choi PC, Chan AW, Chim AM, Yiu KK, Chan FK, Sung JJ, Wong VW. Alanine aminotransferase-based algorithms of liver stiffness measurement by transient elastography (Fibroscan) for liver fibrosis in chronic hepatitis B. J Viral Hepat. 2009 Jan;16(1):36-44.

[123] Papatheodoridis GV, Manolakopoulos S, Liaw Y, Lok A. Follow-up and indications for liver biopsy in HBeAg-negative chronic hepatitis B virus infection with persistently normal ALT: A systematic review. Journal of Hepatology 2012 vol. 57 j 196–202.

[124] Colecchia A, Montrone L, Scaioli E, et al. Measurement of spleen stiffness to evaluate portal hypertension and the presence of esophageal varices in patients with HCV-related cirrhosis. Gastroenterology 2012;143:646-654.

[125] Sharma P, Kirnake V, Tyagi P, et al. Spleen stiffness in patients with cirrhosis in predicting esophageal varices. Am J Gastroenterol 2013;108:1101-1107.

[126] Takuma Y, Nouso K, Morimoto Y, et al. Measurement of spleen stiffness by acoustic radiation force impulse imaging identifies cirrhotic patients with esophageal varices. Gastroenterology.

[127] Wong GL, Chan HL, Wong CK, et al. Liver stiffness-based optimization of hepatocellular carcinoma risk score in patients with chronic hepatitis B. J Hepatol 2014;60:339-345

[128] Vergniol J, Foucher J, Terrebonne E, et al. Noninvasive tests for fibrosis and liver stiffness predict 5-year outcomes of patients with chronic hepatitis C. Gastroenterology 2011;140:1970-1979.

[129] de Ledinghen V, Vergniol J, Barthe C, et al. Non-invasive tests for fibrosis and liver stiffness predict 5-year survival of patients chronically infected with hepatitis B virus. Aliment Pharmacol Ther 2013;37:979-988.

[130] Parkes J, Roderick P, Harris S, et al. Enhanced liver fibrosis test can predict clinical outcomes in patients with chronic liver disease. Gut 2010;59:1245-1251.

[131] Karlas T, Petroff D, Garnov N, Bo S, Tenckhoff H, Wittekind C, Wiese M, Schiefke I, Linder N, Schaudinn A, Busse H, Kah T, Mössner J, Berg T, Tröltzsch M, Keim V, Wiegand J. Non-Invasive Assessment of Hepatic Steatosis in Patients with NAFLD Using Controlled Attenuation Parameter and 1H-MR Spectroscopy PLOS ONE March 2014 | Volume 9.

[132] Myers RP, Pollett A, Kirsch R, Pomier-Layrargues G, Beaton M, et al. (2012) Controlled Attenuation Parameter (CAP): a noninvasive method for the detection of hepatic steatosis based on transient elastography. Liver Int 32: 902–910.

[133] Fujii Y, Taniguchi N, Itoh K, Shigeta K, Wang Y, Tsao JW, Kumasaki K, Itoh T. A new method for attenuation coefficient measurement in the liver: Comparison with the spectral shift central frequency method. J Ultrasound Med 2002;21:783–788.

[134] Garra BS, Insana MF, Shawker TH, Russell MA. Quantitative estimation of liver attenuation and echogenicity: Normal state versus diffuse liver disease. Radiology 1987;162:61–67.

[135] Shi KQ, Tang JZ, Zhu XL, Ying L, Li DW, Gao J, Fang YX, et al. Controlled attenuation parameter for the detection of steatosis severity in chronic liver disease: a meta-analysis of diagnostic accuracy. J Gastroenterol Hepatol 2014;29:1149–1158.

[136] Shen F, Zheng RD, Shi JP, Mi YQ, Chen GF, Hu X, Liu YG, et al. Impact of skin capsular distance on the performance of controlled attenuation parameter in patients with chronic liver disease. Liver Int 2015;35:2392–2400.

[137] de Ledinghen V, Vergniol J, Capdepont M, Chermak F, Hiriart JB, Cassinotto C, Merrouche W, et al. Controlled attenuation parameter (CAP) for the diagnosis of steatosis: a prospective study of 5323 examinations. J Hepatol 2014;60:1026–1031.

[138] Kwok R, Choi KC, Wong GL, Zhang Y, Chan HL, Luk AO, Shu SS, et al. Screening diabetic patients for non-alcoholic fatty liver disease with controlled attenuation parameter and liver stiffness measurements: a prospective cohort study. Gut. 2016;65:1359–1368.

[139] Sasso M, Audiere S, Kemgang A, Gaouar F, Corpechot C, Chazouilleres O, Fournier C, et al. Liver steatosis assessed by controlled attenuation parameter (cap) measured with the XL probe of the FibroScan: a pilot study assessing diagnostic accuracy. Ultrasound Med Biol 2016;42:92–103.

[140] Yilmaz Y, Ergelen R, Akin H, Imeryuz N. Noninvasive detection of hepatic steatosis in patients without ultrasonographic evidence of fatty liver using the controlled attenuation parameter evaluated with transient elastography. Eur J Gastroenterol Hepatol 2013;25:1330–1334.

[141] Petta S, Wai-Sun Wong V, Hiriart JB, Lai-Hung Wong G, Marra M, Vergniol J, Wing-Hung Chan A, Di Marco V, Merrouche W, Lik-Yuen Chan H, Barbara M, Le-Bail B, Arena U, Crax A and de Ledinghen V. Improved Noninvasive Prediction of Liver Fibrosis by Liver Stiffness Measurement in Patients With Nonalcoholic Fatty Liver Disease Accounting for Controlled Attenuation Parameter Values. Hepatology 2017;65:4.